

**STABILITY ANALYSIS OF SOLAR TRACKING SYSTEM
THROUGH CONVENTIONAL CONTROLLERS**

A thesis report

Submitted in the partial fulfillment of the requirements for the award of

Degree of

Master of Engineering

In

Electronics Instrumentation & Control Engineering

Submitted By:

Rahul Garg

Roll No.801151020

Under the supervision of:

Dr. Gagandeep Kaur

Assistant Professor



**DEPARTMENT OF ELECTRICAL AND INSTRUMENTATION
ENGINEERING THAPAR UNIVERSITY**

JULY 2013

DEDICATED


TO

MY PARENTS


CERTIFICATE

I hereby certify that the work which is presented in the thesis entitled "Stability Analysis of Solar Tracking System Through Conventional Controllers" in partial fulfillment of the requirements for the award of degree of Master of Engineering in Electronics Instrumentation and Control Engineering at Thapar University, Patiala, is an authentic record of my own work carried out under the guidance and supervision of **Dr. Gagandeep Kaur** (Assistant Professor) and refers other researcher's works which are duly listed in the reference section. The matter embodied in this report has not been submitted anywhere for the award of any degree.


Date: 15/7/13



Rahul Garg
Roll No. 801151020

It is certified that the above statement made by the student is correct to the best of our knowledge and belief.


Dr. Gagandeep Kaur
Assistant Professor, EIED
Thapar University, Patiala

Countersigned By


Dr. Smarajit Ghosh
Head of Department
Department of the Electrical and
Instrumentation Engineering,
Thapar University, Patiala, Punjab.


Dr. S.K. Mohapatra
Dean of Academic Affairs
Thapar University, Patiala
Punjab

ACKNOWLEDGEMENT

The real spirit of achieving a goal is through the way of excellence and austere discipline. I would have never succeeded in completing my task without the cooperation, encouragement and help provided to me by various personalities.

First of all I render my gratitude to the ALMIGHTY who bestowed self-confidence, ability and strength in me to complete this work. Without his grace this would never have been today's reality.

With deep sense of gratitude I express my sincere thanks to my esteemed and worthy supervisor **Dr. Gagandeep kaur** for his invaluable guidance. It would have never been possible to complete this work without his continuous support and encouragement. In spite of his very busy schedule he was always approachable and available to attend to my problems, discuss the solutions and give the appropriate advice. Doing research under his supervision was a very enlightening and enjoyable experience.

I also wish to thank all the faculty members of the Department of Electrical and Instrumentation Engineering for the invaluable knowledge they have imparted on me and for teaching the principles in most exciting and enjoyable way.

I also extend my thanks to the technical staff of the department for maintaining an excellent working facility.

I would like to thank my parents for supporting and taking me to this stage in life; it was their blessings which always gave me courage to face all challenges and made my path easier.

RAHUL GARG

Roll No.801151020

ABSTRACT

Solar energy is considered to be as a renewable energy solution for most of energy crises and environmental pollutions and it is Proportional integral derivatively advancing as an important means of renewable energy resource. The main purpose of a solar tracking system is to track the movement of the sun during the sunshine in order to orientate the solar panel to the maximum radiation in all time. More energy is produced by tracking the solar panel to remain aligned to the sun at a right angle to the rays of light.

This thesis describes in detail the design modeling and stability of a solar tracking system through conventional controllers of a prototype for solar tracking system. In this thesis the torque of the servo motor used for a single axis solar tracker as well as the selection criteria of a servomotor used for the tracker is calculated. The effect of the wind (first order), cloud (second order) and rain (third order) as a disturbance on the solar tracker is also considered. Finally the solar tracker and disturbance transfer functions have been developed using experimental data. After the mathematical modeling the control objective is set and different kind of conventional controllers are designed to meet the control objective. Firstly Feedback controller and then feedback plus feed forward controller are implemented to meet the control objective but due to their limitations these controllers were unable to give satisfactory results. So a model based controller is designed which has only one tuning parameter as compared to three tuning parameters of Proportional integral derivative controller. The model based controller gives a satisfactory result.

TABLE OF CONTENTS

CONTENTS

Certificate

Abstract

Acknowledgement

Table of Contents

List of Figures

Chapter1: Introduction

1.1 Overview	1
1.2 Motivations	1
1.3 Objective and Scope	1
1.4 Organization	2
1.5 Literature Survey	2-5

Chapter2: System modeling of solar tracking system

2.1 Introduction	7
2.2 Control system design	7-10
2.3 Calculations required for system modeling	10-15
2.4 Mathematical modeling	16-19

Chapter3: Tuning of PROPORTIONAL INTEGRAL DERIVATIVEand its implementation for proposed system

3.1 Control of Solar Tracking System

3.2 Hand geometry system

3.2.1 Image Acquisition

3.2.2Image Preprocessing

3.3.3 Hand Feature Extraction

3.3.4Matching

3.3.5Decision

3.3.6 Algorithm

Chapter4: Experimental Results

Chapter5: Conclusion and future work

Chapter6: References

List of Table

Table 3.1: The main selected motor parameters

Table 3.2: Effects of increasing a parameter independently

Table 3.3: Ziegler - Nicholas method

List of Figures

Figure 3.1: Simplified block diagram of solar tracking system

Figure 3.2: One axis sun tracking system

Figure 3.3: The time speed curve

Figure 3.4: The speed torque curve of the selected motor and the required system torque

Figure 3.5: The suggested perpendicular azimuth axis solar tracker

Figure 3.6: The trapezoidal move profile.

Figure 3.7: The transfer function model of solar tracking system

Figure 3.8: Reduced transfer function model of solar tracking system

Figure 3.9: Unit step response of the process at different values of gain

Figure 4.1: Block diagram of PROPORTIONAL INTEGRAL DERIVATIVE controller

Figure 4.2: The step response of the process at the value of gain $K= 131415$.

Figure 4.3: Simulink model with PROPORTIONAL INTEGRAL DERIVATIVE controller including disturbance due to wind.

Figure 4.4: Unit step response of figure 4.3

Figure 4.5: Simulink model with PROPORTIONAL INTEGRAL DERIVATIVE controller including disturbance due to cloud.

Figure 4.6: Unit step response of figure 4.5

Figure 4.7: Simulink model with PROPORTIONAL INTEGRAL DERIVATIVE controller including disturbance due to rain.

Figure 4.8: Unit step response of figure 4.7

Figure 4.9: Feedback plus feedforward controller including disturbance due to wind.

Figure 4.10: Unit step response of figure 4.9

Figure 4.11: Feedback plus feedforward controller including disturbance due to cloud.

Figure 4.12: Unit step response of figure 4.11

Figure 4.13: Feedback plus feedforward controller including disturbance due to rain.

Figure 4.14: Unit step response of figure 4.13

Figure 5.1: Open loop control strategy

Figure 5.2: Schematic of the IMC scheme

Figure 5.3: Rearrangement of IMC block diagram

Figure 5.4: IMC reduced to conventional block diagram

Figure 5.5: Simulink based IMC for first order

Figure 5.6: Unit step response of fig 5.5

Figure 5.7: Simulink based IMC for second order

Figure 5.8: Unit step response of fig 5.7

Figure 5.9: Simulink based IMC for third order

Figure 5.10: Unit step response of fig 5.9

INTRODUCTION

1.1 Overview

In this thesis mathematical modeling of solar tracking system through available experimental data and its stability analysis through different conventional controllers have been developed and designed using the MATLAB/Simulink for tracking a solar energy module in order to achieve its optimal operational efficiency. The input data provided to the designed control system in form of the altitude angle is obtained from the solution of a system of governing equations which describe the movement of the sun from the sunrise to the sunset. The optimum performance of the designed tracking system can be achieved if the angle of incidence is equal to zero during the sunshine. In such case the solar energy acquired by the system is maximized. After simulation of the model control of the model is necessary. There are different ways to control a solar tracking system. This thesis gives a brief idea of different controlling techniques and different aspects of controller design for a control system taken in to consideration.

1.2 Motivation

Control systems are inherently time domain systems subject to time varying inputs and are to be analyzed and tested using time domain test signals like unit step signal. The controllers are the backbone of all the controls in the industries since the first control system came in to design. After the design of controller is performed; the performance evaluation part comes in to light. The designed controller has to give optimum control results irrespective of every situation like system non linearity effects of disturbances and system saturation.

1.3 Objective and scope of the thesis

The objective of this thesis is to determine the stability analysis of the solar tracking system by designing the conventional controllers. To determine the controller characteristics the time response and frequency response is carried out. Although there are other controllers like

intelligent controllers but they are complex in design so in this emphasis is laid mainly on conventional controllers. The other objective of the thesis is to find out the key design challenges in design of conventional controllers.

1.4 Organization of thesis

Chapter 2 describes the design and factors considered during mathematical modeling of solar tracking system with the use of experimental data. It also represents the transfer function model of the desired control system.

Chapter 3 describes the designing methods of PROPORTIONAL INTEGRAL DERIVATIVE controller by Ziegler Nichols tuning and then for better performance the feedback and feedback plus feed forward controller is designed and their characteristics is compare

Chapter 4 describes the internal modal controller and its designing for better evaluation of desired control system

Chapter 5 describes the results and the concluding remarks of this thesis and the future work which can be taken in to consideration.

LITERATURE SURVEY

The following section describes the literature survey that is relevant with the work carried out for this thesis work.

M. Kamal et al in his paper presented system modeling is a key element in process control. Applying the many methods of control to improve command response stability and disturbance rejection requires an understanding of the system under control. Also for the solar tracking systems the choice of driving motors gears amplifiers as well as the position detectors is very important step in an active system design. In the present paper the torque of the servo motor used for a single axis solar tracker under Egypt climate as well as the selection criteria of a servomotor used for the tracker are calculated. The effect of the wind on the solar tracker in Egypt has been considered. Finally the solar tracker and disturbance transfer functions have been developed [1].

Erik Liedholm et al in his thesis deals with the problem of attaining high power output from solar panels by employing a maximum power point tracker. The purpose being to propose a viable technique that tracks the maximum power point using only voltage measurements as well as investigating the possibility to control several solar panels individually employing only one actuator. Using a custom measurement circuit and a data acquisition device connected to a Lab view program the characteristics of eight solar panels were monitored for a month. The measurement data was then used in Matlab simulations to evaluate a specific maximum power point tracker called incremental conductance. Some other tracking algorithms were also studied but only the most promising one was implemented. The incremental conductance algorithm was successfully implemented using only voltage measurements and 94.74% of the electrical power from the solar panels throughout January 2010 was harvested in the most prosperous simulation. Further using only one actuator to control four solar panels at their individual maximum power points was shown to be possible [2].

Ashraf Baalbek et al in his paper he presented mathematical analysis control system and Simulink model have been developed designed and tested using the MATLAB/Simulink for

tracking a solar energy photo/voltaic module in order to achieve its optimal operational efficiency. The input data provided to the designed control system in form of the altitude angle is obtained from the solution of a system of governing equations which describe the movement of the sun from the sunrise to the sunset. The optimum performance of the designed tracking system can be achieved if the angle of incidence is equal to zero during the sunshine. In such case the solar energy acquired by the system is maximized. The obtained results show the simplicity accuracy and applicability of the present designed controller to meet all operational requirements. Moreover the proposed tracking system can be used either for educational or research purposes [3].

Subhranshu et al in his paper presented the performance evaluation of different conventional and Intelligent Controllers for Temperature Control of Shell and Tube Heat Exchanger System[4].

Mirciea Grigoriu et al in his paper presented the electricity generated from renewable sources is becoming more available. The choice of such renewable energy sources for consumers to support the development of clean energy that will reduce the environmental impacts associated with conventional energy generation and increase energy independence. To increase the efficiency of a photovoltaic panel that is facing the sun agreed thus achieving a system for tracking the position of the sun. Via a preprogrammed trajectory to have the sun according to the hours of the day [5].

Samar Alsadi et al in his paper deals with a simulation study of maximum power point tracking (MPPT) for photovoltaic systems using perturb and observe algorithm. Maximum power point tracking (MPPT) plays an important role in photovoltaic systems because it maximize the power output from a PV system for a given set of conditions and therefore maximize the array efficiency and minimize the overall system cost. Since the maximum power point (MPP) varies based on the irradiation and cell temperature appropriate algorithms must be utilized to track the (MPP) and maintain the operation of the system in it. Matlab/Simulink is used to establish a model of photovoltaic system with (MPPT) function. This system is developed by combining the models established of solar PV module and DC-DC Boost converter. The system is simulated under different climate conditions. Simulation results show that the photovoltaic simulation system can track the maximum power point accurately. A particular typical 50W solar panel was used for model evaluation and results of simulation were

compared with points taken directly from the data sheet and curves published by the manufacturers[6].

M. A. Usta et al presented in his paper a solar tracking system which is designed to optimize the operation of solar energy receivers. More solar energy is collected by the end of the day if solar receivers are installed with a tracker system. In this paper a solar tracking system is modeled using Matlab/Simulink and a fuzzy logic control is designed for the control of this system. The generated controller was combined with the solar tracking system and the control was realized with the fuzzy logic controller in the Matlab/Simulink environment. At the same time PI control is applied to the system and the results obtained with PI control were compared with the results of fuzzy logic [7].

Qinhao Zhang et al in his paper propose adaptive control architecture for maximum power point tracking (MPPT) in photovoltaic systems. To improve the performance of MPPT this paper develops a two level adaptive control architecture that can reduce complexity in system control and effectively handle the uncertainties and perturbations in the photovoltaic systems and the environment. The first level of control is ripple correlation control (RCC) and the second level is model reference adaptive control (MRAC).By decoupling these two control algorithms the system achieves MPPT with overall system stability. This paper focuses mostly on the design of the MRAC algorithm which compensates the under-damped characteristics of the power conversion system. The original transfer function of the power conversion system has time-varying parameters and its step response contains oscillatory transients that vanish slowly. Using the Lyapunov approach an adaption law of the controller is derived for the MRAC system to eliminate the under-damped modes in power conversion. It is shown that the proposed control algorithm enables the system to converge to the maximum power point in milliseconds [8].

Khuzairaybin et al presented in his thesis solar tracking system that used PIC16F877A microcontroller as a brain to control the whole system. The LDR (Light Dependent Resistor) had been used to sense the intensity of light at 30 degree each or 180 degree total and sent the data to the microcontroller. This microcontroller will compare the data and rotate a stepper motor to the right direction. The stepper motor will rotate the solar panel based on the highest intensity of light [9].

Nader Barsoum et al in his paper presented solar energy are aProportional integral derivatively advancing as an important means of renewable energy resource. More energy is produced by tracking the solar panel to remain aligned to the sun at a right angle to the rays of

light. This paper describes in detail the design and construction of a prototype for solar tracking system with two degrees of freedom which detects the sunlight using photo cells. The control circuit for the solar tracker is based on a PIC16F84A microcontroller (MCU). This is programmed to detect the sunlight through the photocells and then actuate the motor to position the solar panel where it can receive maximum sunlight [10].

Priyanka et al presented in her thesis presented the modeling of nonlinear current-voltage characteristics of solar cells for performance prediction becomes difficult under the influence of shading. Non-uniform illumination due to shadows casted by the other panels/modules buildings clouds etc. can cause maximum power to change drastically. Partial shading of PV installations has a disproportionate impact on its power production. Moreover the power losses in the individual shaded cells would result in local heating and create thermal stress on the entire module/array resulting in hot-spot formation. Under extreme cases of shading the reverse bias on the solar cell might exceed its breakdown voltage and cause irreparable damage [11].

Khuzairy Bin et al presented in his thesis solar tracking system that used PIC16F877A microcontroller as a brain to control the whole system. The LDR (Light Dependent Resistor) had been used to sense the intensity of light at 30 degree each or 180 degree total and sent the data to the microcontroller. This microcontroller will compare the data and rotate a stepper motor to the right direction. The stepper motor will rotate the solar panel based on the highest intensity of light [12].

Osman Hassan et al in his paper presented the accuracy of control systems analysis is of paramount importance as even minor design flaws can lead to disastrous consequences in this domain. This paper provides a higher-order-logic theorem proving based framework for the formal analysis of steady state errors in feedback control systems. In particular in this paper it is presented the formalization of control system foundations like transfer functions summing junctions feedback loops and pick off points and steady state error models for the step ramp and parabola cases. These foundations can be built upon to formally specify a wide range of feedback control systems in higher-order logic and reason about their steady state errors within the sound core of a theorem prove. The proposed formalization is based on the complex number theory of the HOL Light theorem proves. For illustration purposes it is presented the steady state error analysis of a solar tracking control system [13].

CHAPTER 3

MODELING OF SOLAR TRACKING SYSTEM

3.1 Introduction

The solar tracker is a system which follows the path of the sun and keeps the sun's rays normal to the solar collector surface all time. The sun's location in the sky relative to a point on the surface can be defined with two angles the solar altitude angle and the solar azimuth angle. These angles are calculated through sun- earth relations [1].Sun tracking is essential for many solar energy based power systems to improve the system performance. It is essential for concentrator systems moreover in flat-plate photovoltaic systems an increase in power output by 30-60% depending on the location has been observed by the tracking as compared to the fixed tilt [2].The solar collectors are mounted on the tracker surface. The solar trackers may be single or double axis trackers but in this thesis the single axis trackers are considered only. There are several common implementations of single axis trackers. These include horizontal single axis trackers perpendicular azimuth single axis trackers tilted single axis trackers and polar aligned single axis trackers. In the present study only the perpendicular azimuth axis tracker is considered [3].and now in this section the single axis solar tracker is briefly discussed along with its modeling assumptions and the available governing mathematical equations required in order to obtain the transfer function model of proposed system.

3.2 System design

In order to move the solar tracker system in particular direction the electric motor as a prime mover is used for motion control. In solar tracking system design any light sensitive device can be used as input sensor unit to detect and track the sun position based on sensors readings and generated sun tracking error the control unit generates the voltage used to command the circuit to drive the motor that outputs the rotational displacement of electric motor which is

the motion of solar tracking system. Simplified block diagram representation of solar tracking system is shown in Fig.3. 1.

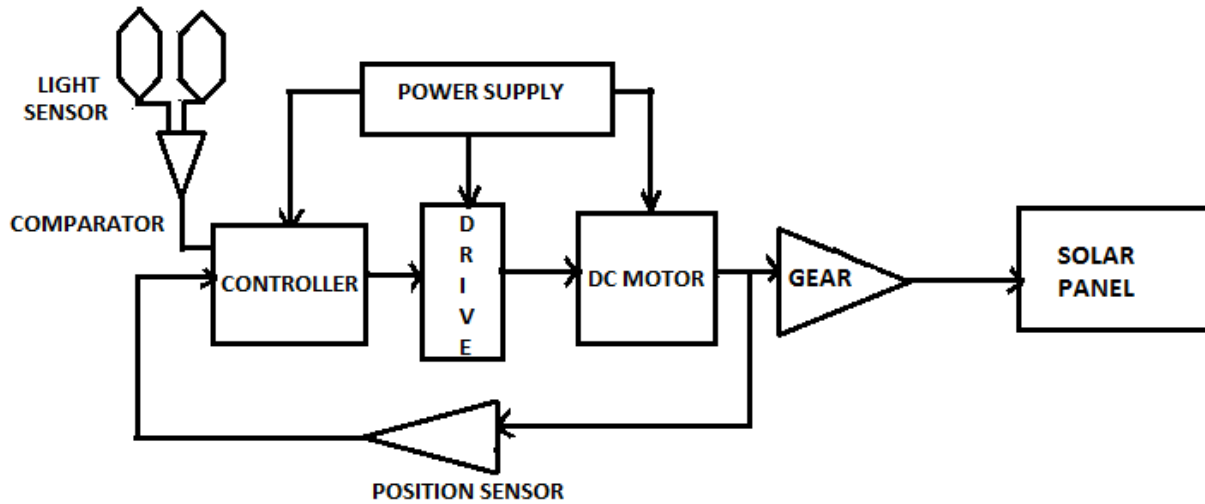


Fig 3.1 Simplified block diagram of solar tracking system [4].

3.2.1. Light sensor selection and circuit:

Light sensors a suitable inexpensive simple and easy to interface sensor is analog LDR. Depending on particular application and required maximum energy receiving of solar panel two main solar tracking system arrangements; one-axis /one directional sun tracking system using two light detectors sensors are mounted on the solar panel and placed in an enclosure the LDR is screened from each other by opaque surfaces. For one-axis sun tracking system one light tracking circuit consisting of two sensors and one electric motor is used.

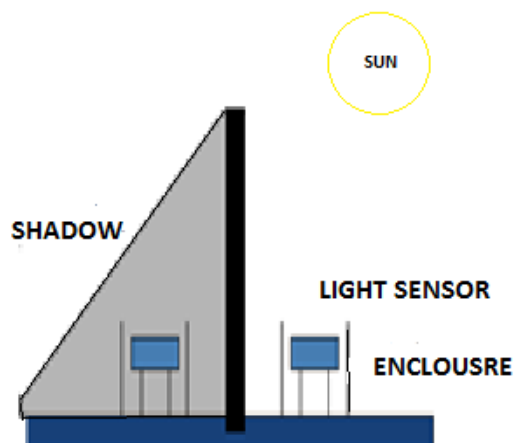


Fig. 3.2 One axis sun tracking system [4]

3.2.2 Actuator and drive selection:

Electric motors most used for solar tracker are permanent magnet digital current and stepper motors; the proper selection of motor and drive combination can save energy and improve performance. A suitable available easy to control and interface selection is PMDC motor [5]. The main selected motor parameters are listed in table 1.

Table 3.1: The main selected motor parameters [3]

Parameter	Value
Low speed torque	0.13 NM
Back emf constant k_b	$50.6 \times 10^{-3} \text{V/rad/Sec}$
Viscous friction coefficient f_m	$3.2 \times 10^{-6} \text{NM/rad/Sec}$
Coulomb friction torque	0.007 NM
Armature inductance I_a	0.001 H
Inertia of the motor j_m	$5.8 \times 10^{-6} \text{kg.m}^2$
Armature resistance R_a	1.93 Ω
Motor Mass	0.49 Kg.

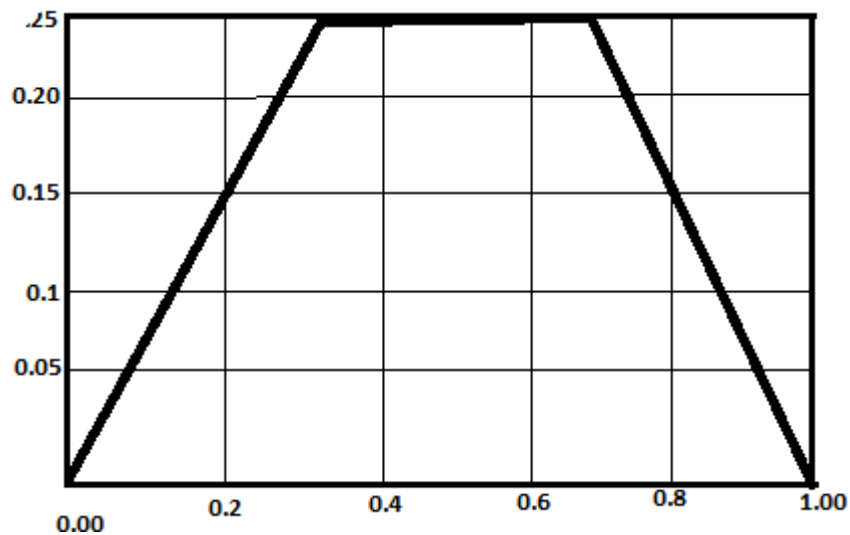


Fig 3.3 The time speed curve[3]

The peak torque required by the application must fall within the peak torque rating of the motor at the peak speed. Fig 3 shows the obtained system speed graph based on the system design.

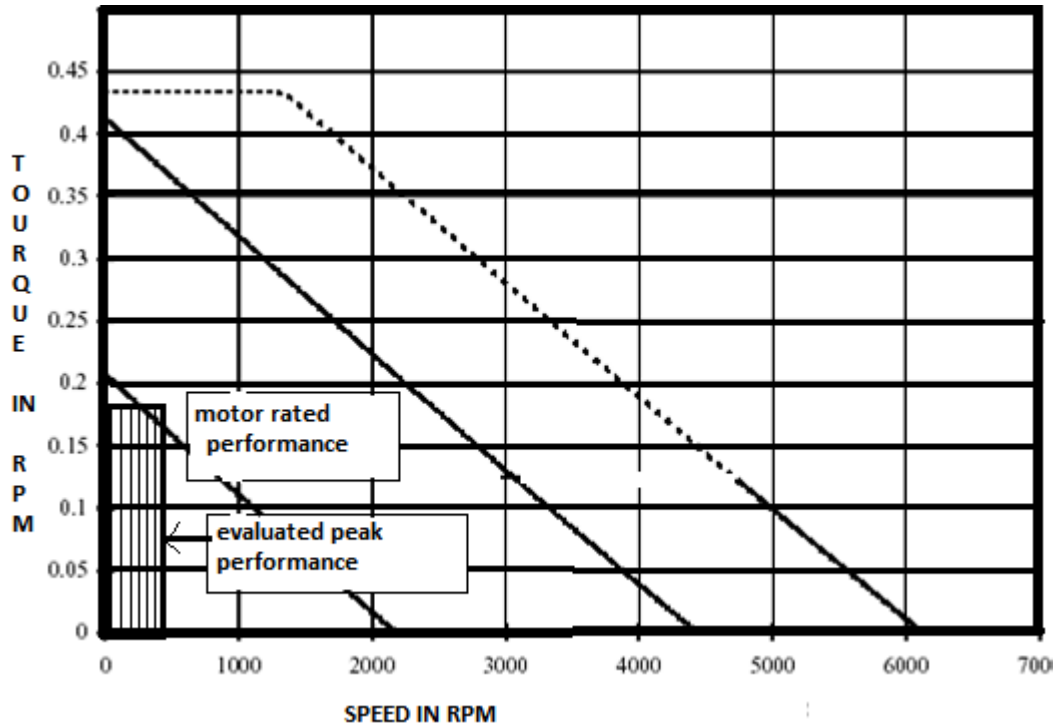


Fig 3 4: The speed torque curve of the selected motor and the required system torque [6].

Fig 3.4 shows the speed torque curve of the selected motor and the required system torque. The maximum required torque by the application is 0.1 NM at $\dot{\omega} = 250$ RPM this falls within the speed/torque of the selected motor as shown in Fig. 4. The safety margin is more than 74% that is enough for the additional constant low friction viscous and other disturbance torques where 20% is minimum enough safety margin [6].

3.3 Calculations and assumptions used for system modeling

In the present study only the perpendicular azimuth axis tracker is considered. For the proposed azimuth axis tracker the total torque acting on the tracker is the sum of the motor torque and load torque. The load torque of moving system has the following components which are reflected to the motor shaft is:

$$T_l = T_j + T_f + T_d \quad (1)$$

The inertial torque T_j is the torque to accelerate and decelerate the load while the frictional torque T_f due to static frictions of the mechanical system. T_d is the viscous damping torque which is proportional to the speed and it is small because the required speed of system is small. At normal operating conditions both T_f and T_d are small and constant. In most cases the inertial torque demands are the peak torque during acceleration. The accelerating torque is proportional to the inertia [7]

$$T_i = j \cdot \alpha \quad (2)$$

3.3.1 Wind forces on the solar collector

It is estimated that the region which is rich with wind has annual average speeds between 5.6 m/s and 8.25 m/s [8]. Then the system torque calculations at wind velocity 10 m/s are suitable to work at this environment. The following section describes the pressure lift drag and moment effects on two dimensional structure forms.

The air flow will develop local pressure P over the body [9]

$$P = 0.5 \rho v^2 \quad (3)$$

The integration of the pressures over the body surface results in a net force and a moment. The net wind pressures forces F_{lift} and F_{drag} in the lift and drag direction respectively are

$$F_{lift} = 0.5 C_{lift} \rho v^2 a \quad (4)$$

$$F_{drag} = 0.5 C_{drag} \rho v^2 a \quad (5)$$

The drag force is the component of the force along flow and the across flow component direction is the lift force.

The net flow-induced moment J is

$$J = 0.5 C_{moment} \rho v^2 A_{ref} L_{ref} \quad (6)$$

A_{ref} is a reference area generally selected to be representative of a plane area subjected to the flow by the body here chosen as the aperture area of a collector module aperture. L_{ref} is a reference length selected to be representative of a characteristics body dimension. The Perpendicular Azimuth Axis Solar Tracker Components as shown in Fig. 5 are:

1. D.C. motor with Pulleys and belts or Roller-chain.
2. The east-west motor aluminum stand.
3. Gear-box.
4. The north-south motor aluminum stand.

5. Box contains the bearings of rotations and the fixing of the horizontal pipe with the stand.
6. The perpendicular aluminum tube of the collector stand.
7. The parallel aluminum tube of the collector stand.
8. The elevation tracking axle.
9. The azimuth tracking vertical axle.
10. The pylon.

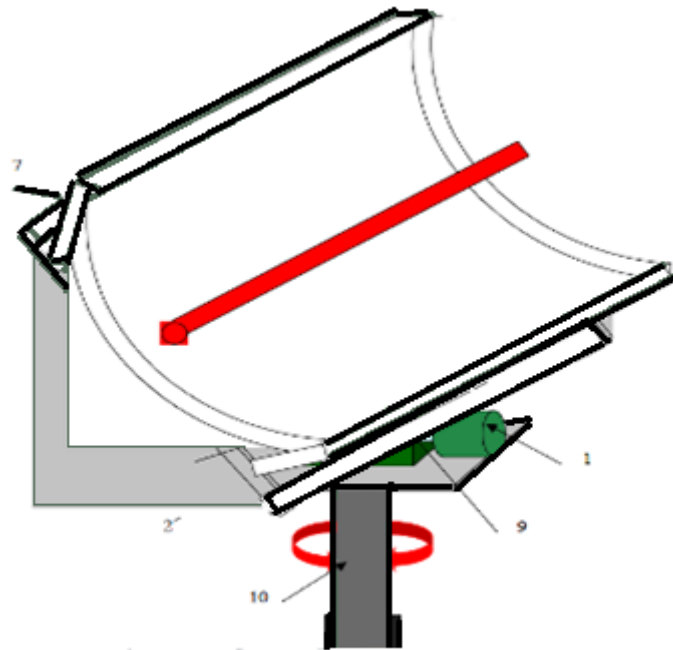


Fig 3.5: The suggested perpendicular azimuth axis solar tracker [3]

3.4 Calculation of moment of inertia

For the perpendicular azimuth axis solar tracker shown in Fig. 5 it is obvious that there are three components contribute significantly for the moment of inertia as follows;

- a) the elevation axis
- b) the load stand
- c) the load (solar collector)

3.4.1 Mass moment of inertia of the horizontal pipe

The geometry of the horizontal pipe is a hollow cylinder with the inner radius of 10.16 cm the thickness is 0.45 cm and the length is 200 cm while the weight of the aluminum pipe is 2.769 kg/m. The pipe mass's moment of inertia is [10].

$$J_{\text{pipe}} = \frac{W * (r_o^2 - r_i^2)}{2} = 0.0011 \text{ kg.m}^2 \quad (8)$$

3.4.2 Mass moment of inertia of the collector stand

The designed collector stand consists of two interconnected aluminum rectangular tubes that are perpendicular to the horizontal pipe with dimensions of 2.54 cm X 5cm as width and 0.318cm X 200cm as length. And the two tubes that parallel to the horizontal pipe with the same dimensions but spaced from the axis of rotation by a distance of 97 cm. The weight of the tube is 0.861 kg /m. The moment of inertia of the two interconnected aluminum rectangular tubes that are perpendicular to the horizontal pipe ($J_{\text{tube-perpend}}$) can be calculated as follows [10]

$$J_{\text{tube-perpend}} = \frac{W * (l^2 + D^2)}{12} = 1.147 \text{ kg.m}^2 \quad (9)$$

By parallel axis theorem the moment of inertia of any object about an axis parallel to its axis but a distance d away ($J_{\text{tube-parallel}}$) is [10]

$$J_{\text{tube-parallel}} = 3.245 \text{ kg.m}^2 \quad (10)$$

3.4.3 The moment effects of the wind disturbance on the tracker

The torque loads that are acting on PTC are wind load and gravity load [11]. For a parabolic trough collector in an array protected with a wind screen fence drag and lift force and moment coefficients equal respectively to 0.5 + 0.5 + 0.35. Air density is 1.229 kg/m³ [12]. Our suggested tracker is ground mounted and the reference area A_{ref} and l_{ref} of the parabolic trough solar collector are 3.5 m² and 1.46 m respectively [13]. Using Eq.(6) at wind velocity 10 m/s then the additional wind load Inertia is:

$$J_{\text{load-wind}} = 525.82 \text{ Kg.m}^2 \quad (11)$$

3.4.4 Mass Moment of Inertia of the Collector

It is considered here a parabolic trough collector with 0.73 m radius 2.4 m length and 30 kg light[14]. The geometry of the PTC is approximated by half thin walled hollow cylinder and the axis of rotation through end. The collector inertia is [10]

$$J_{\text{load-collector}} = 3.675 \text{ Kg.m}^2 \quad (12)$$

3.4.5 The load torque calculations

The total load inertia is [3]

$$J_{\text{load}} = J_{\text{pipe}} + J_{\text{tube-perpend}} + J_{\text{tube-parallel}} + J_{\text{load_collector}} + J_{\text{load_wind}} \quad (13)$$

By putting the values obtained all the parameters in above equation obtained the value of total load i.e. 533.892 kg.m².

The load angular velocity and displacement respectively $\dot{\omega}_1$ and theta can be described by means of move profile graphs as shown in Fig. 6 which shows the trapezoidal move profile [11].

$$\dot{\omega}_1 = 0.25 \text{ RPM} \quad (14)$$

The peak acceleration $\alpha = 1.175 \text{ rad/sec}^2$

From Eq. (2) the acceleration torque is

$$T_1 = J\alpha = 62.372 \text{ Nm} \quad (15)$$

Selecting a gear-reducer ratio $n = 1/1000$ then the reflected acceleration torque with the assumption that the gear-reducer efficiency=75%

$$T_1 = .01 \text{ Nm} \quad (16)$$

The reflected deceleration torque equals to the reflected acceleration torque. The minimal required motor angular speed is

$$\dot{\omega}_m = 250 \text{ RPM} \quad (17)$$

and the motor HP calculated is = .035 HP[11]

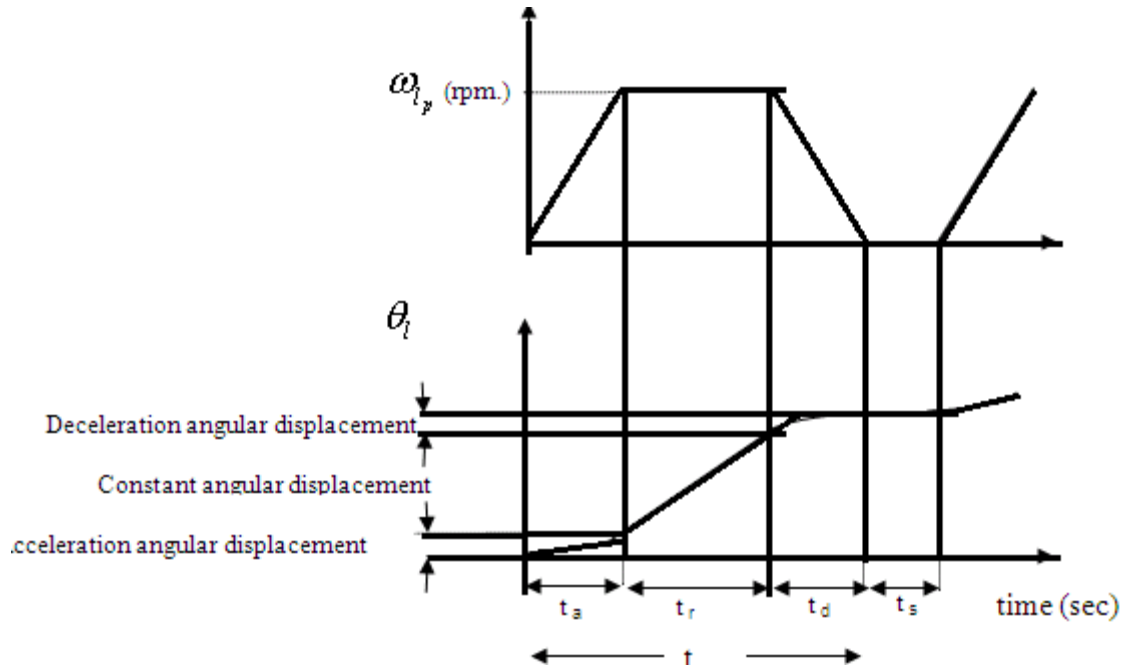


Fig 3.6 The trapezoidal move profile[11]

In Fig 3.6 t_a is defined as the acceleration time t_r as the maximum speed time t_d as the deceleration time and t_s as the off time. With the assumption that $t_a = t_r = t_d$ the peak angular velocity $\dot{\omega}_l$ of the tracking system to move an angular displacement θ in a time equals 1 sec [11].

$$\theta = .0174 \text{ radians} \quad (18)$$

3.5. Mathematical modeling

The Permanent Magnet DC motor is an example of electromechanical systems with electrical and mechanical components. Based on [15-17] the PMDC motor open loop transfer function without any load attached relating the input voltage $V_{in}(s)$ to the output angular displacement $\theta(s)$ is given by Eq.(19). The total equivalent inertia J_{equiv} and total equivalent damping b_{equiv} at the armature of the motor are given by equations given by Eq.(20) for simplicity the solar panel can be considered to be of cuboids shape with the inertia calculated by Eq.(20) correspondingly the equivalent solar tracker system transfer function with load attached and gear ratio n is given by Eq.(21)

$$G_{angle}(s) = \theta(s) / v_{in} = k_m / s [J l_a s^2 + (l_a f + R_a J) s + R_a f + k k_b] \quad (19)$$

$$G_d(s) = \frac{\theta_l(s)}{T_{dist}(s)} = n R_a l_a(s) / [s (J l_a s^2 + (l_a f + R_a J) s + R_a f + k k_b)] \quad (20)$$

The inductance L_a in armature circuit is usually small and may be neglected [3] and then transfer functions have been given by Eqs. (19 20) are reduced to

$$G_{\text{angle}}(s) = k_m/s(\tau_m(s) + 1)$$

$$G_d(s) = -nk_d/s(\tau_m(s) + 1)$$

Based on the open loop reduced transfer function the reduced open loop block diagram is shown in Fig. 7. Using the selected motor parameter in table 1 load inertia in equation (12 and 13) considering the gear ratio n and substitute in Equations (20 21) neglecting the load viscous friction then;

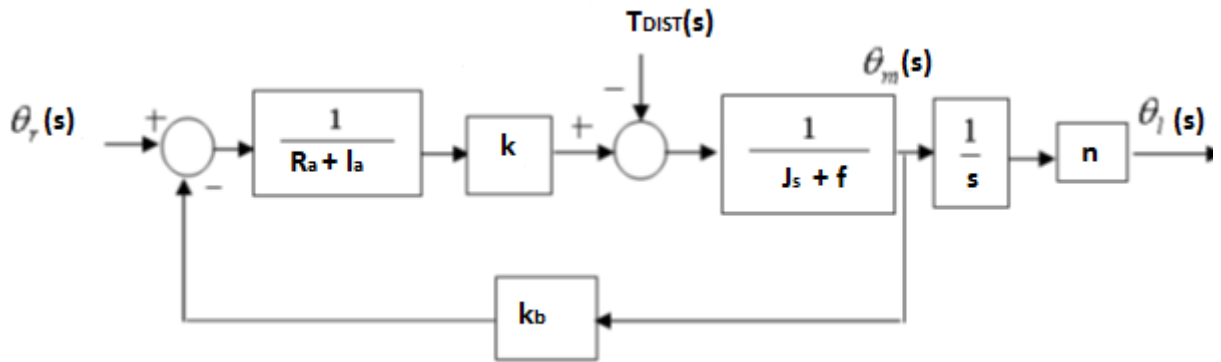


Fig3.7 The transfer function model of solar tracking system

The plant and disturbance transfer functions will be as follows

$$G_p(s) = 0.0197/s(s + 0.401) \quad (22)$$

$$K_b = .16/10s + 1 \quad (23)$$

Based on this calculation with the help of available data the reduced transfer function model block diagram is shown below where k is the critical gain implemented in the forward path of the system.

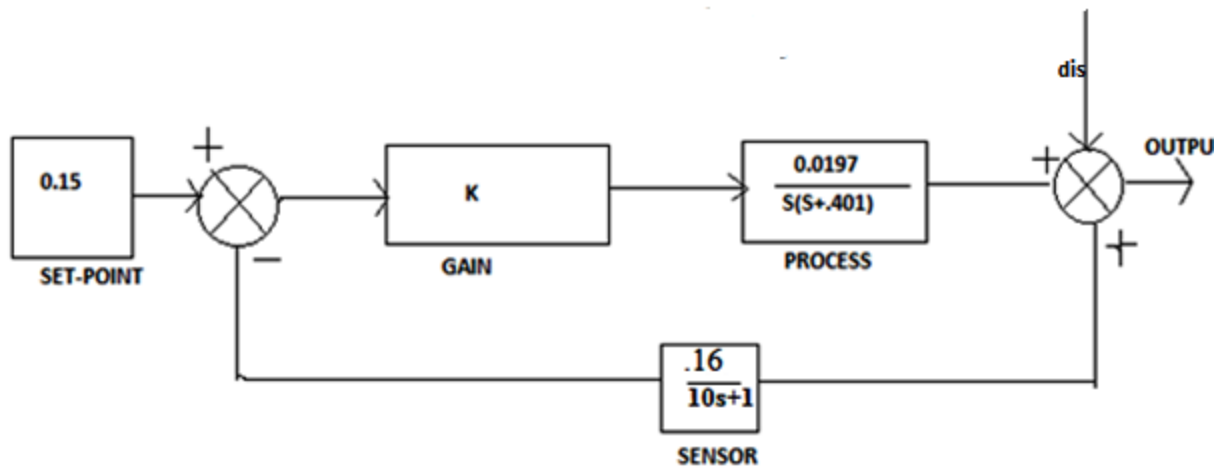


Fig3.8 Reduced transfer function model of solar tracking system

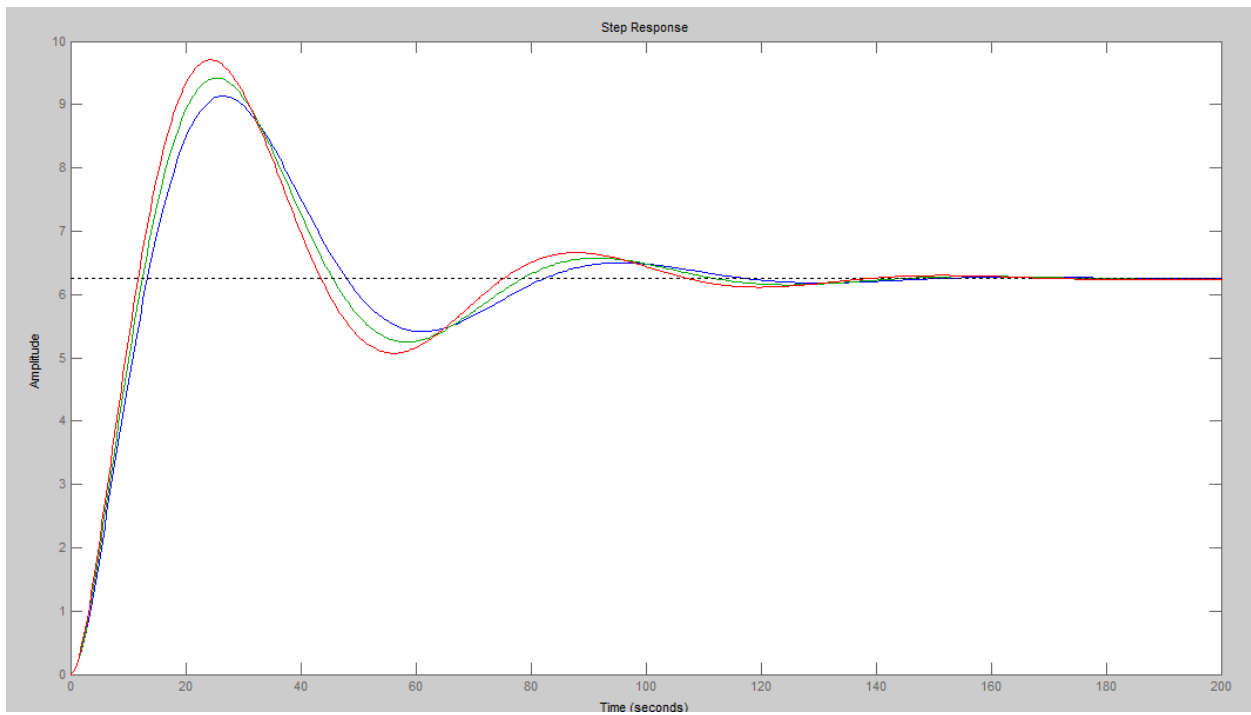


Fig 3.9 Unit step response of the process at different values of gain k=13 14 15

Fig3.9 shows the unit step response of the system at the values of K equal to 13 14 & 15. The unit step response of the transfer function obtained shows that the steady state error and the speed of response is reduced but as the value of gain k increased the system goes unstable .

In fig 3.8 the disturbance transfer function is not shown because disturbances of different kind is considered in this thesis which is discussed in the later chapters and its effect on the system is considered and implemented in Simulink/Matlab

TUNING OF PROPORTIONAL INTEGRAL DERIVATIVE AND ITS IMPLEMENTATION FOR PROPOSED SYSTEM

4.1 Control of solar tracking system

Different assumptions have been made to develop the control model of solar tracking system. Firstly the inductance in the armature coil of motor used is considered very small and is neglected. Secondly the load viscous friction is considered neglected. In this model a potentiometer is used as a positioning sensor in the feedback path when the potentiometer reaches the value corresponding to edge the controller stops the motor and immune it from rotating in that direction. Potentiometer is a sensor used to measure the actual output position the potentiometer constant K_{pot} is equal to the ratio of the voltage change to the corresponding altitude angle change.

In solar tracking system the light detecting sensor is used for detecting sun position .Based on sensor error the controller generates the voltage signal and drives the motor which further outputs the rotational displacement of electric motor which is the motion of solar tracking system. The described below control strategies can be applied for achieving desired solar tracker fast response with minimum error system Simulink model will include these control strategies so the proposed system model can be tested applying any of these control strategies to choose the most suitable control.

4.2 Proportional integral derivative controller

The mnemonic proportional integral derivative refers to the first letters of the names of the individual terms that makeup the standard three-term controller. These are P for the proportional term I for the integral term and D for the derivative term in the controller. Three-term or proportional integral derivative controllers are probably the most widely used industrial controller. Even complex industrial control systems may comprise a control network whose main control building block is a proportional integral derivative control module. The three-term proportional integral derivative controller has had a long history of use and has survived the

changes of technology from the analog era into the digital computer control system age quite satisfactorily. It was the first and only controller to be mass produced for the high-volume market that existed in the process industries. The proportional integral derivative controller calculation consist of three different parameters

and sometimes called three term controller. The proportional value determines the reaction to the current controller the integral value determines the reaction based on the sum of recent error and derivative value determines the reaction based on the rate at which error has been changing.

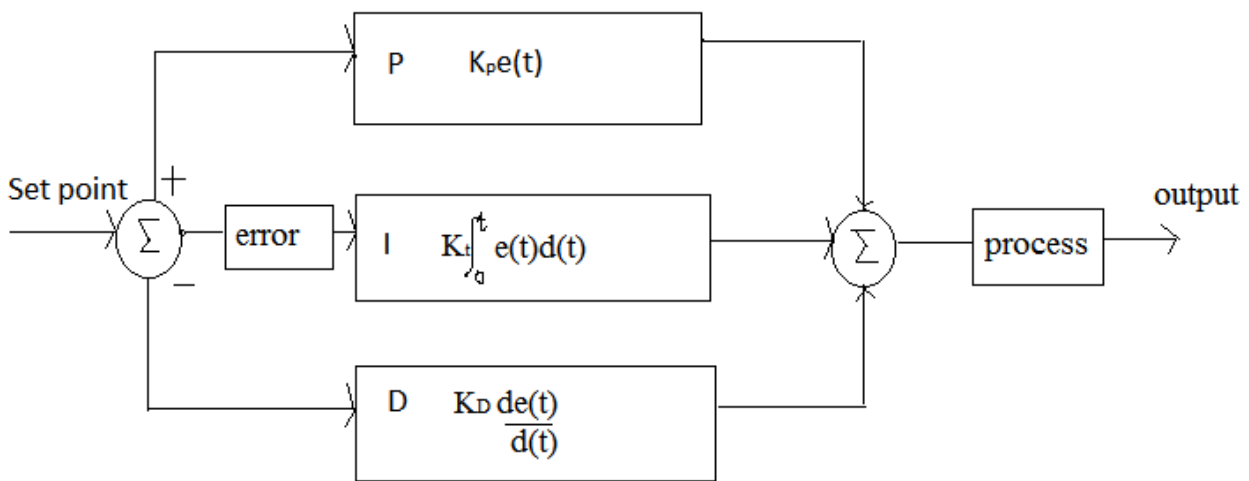


Fig 4.1 Block diagram of proportional integral derivative controller

These values can also be interpreted in terms of time like P represents present error I represents past error and D represents future error. By tuning these three parameters the controller can provide control action designed for the specific process requirement. The response of the controller can be described in terms of an error the degree of which the controller overshoots the set point and the degree of system oscillation. The proportional integral derivative control does not guarantee the optimal stability of the desired process.

4.2.1 Proportional integral derivative control theory

The proportional integral derivative controller is the mostly used in the feedback designed model. If $u(t)$ is the control signal sent to the controller and $y(t)$ is the measured output

and $r(t)$ is the desired output then the tracking error is $e(t) = r(t) - y(t)$ proportional integral derivative controller has the general form:

$$U(t) = k_p e(t) + k_i \int_0^t e(t) dt + k_d \frac{de(t)}{dt} \quad (24)$$

The desired closed loop dynamics can be controlled by the tuning the three parameters i.e. K_p , K_i and K_d . Stability can also be insured by the proportional term. The integral term is used for the rejection of step disturbance and the derivative term is used for the damping or shaping of the response. Sometimes the proportional integral derivative controller is not used for the complex mimo systems.

i) Proportional gain K_p

Larger values typically mean faster response since the larger the error the larger the proportional term compensation. An excessively large proportional gain will lead to process instability and oscillation.

ii) Integral gain K_i

Larger values imply steady state errors are eliminated more quickly. The trade-off is larger overshoot: any negative error integrated during transient response must be integrated away by positive error before reaching steady state.

iii) Derivative gain K_d

Larger values decrease overshoot but slow down transient response and may lead to instability due to signal noise amplification in the differentiation of the error.

4.3 Loop tuning

Tuning a control loop is the adjustment of its control parameters i.e. gain/proportional band integral gain/reset derivative gain/rate to the optimum values for the desired control response. Stability is a basic requirement but beyond that different systems have different behavior different applications have different requirements and some desiderata conflict. Further some processes have a degree of non-linearity and so parameters that work well at full-load conditions don't work when the process is starting up from no load; this can be corrected by gain scheduling. Proportional integral derivative controllers often provide acceptable control even in the absence of tuning but performance can generally be improved by careful tuning and

performance may be unacceptable with poor tuning. Proportional integral derivative tuning is a difficult problem even though there are only three parameters and in principle is simple to describe because it must satisfy complex criteria within the limitations of proportional integral derivative control. There are accordingly various methods for loop tuning and more sophisticated techniques are the subject of patents; this section describes some traditional manual methods for loop tuning.

4.4 Stability

If the Proportional integral derivative controller parameters are chosen incorrectly the controlled process input can be unstable i.e. its output diverges with or without oscillation and is limited only by saturation or mechanical breakage. Instability is caused by excess gain particularly in the presence of significant lag. Generally stability of response is required and the process must not oscillate for any combination of process conditions and set points though sometimes marginal stability is acceptable or desired.

4.5 Optimum behavior

The optimum behavior on a process change or set point change varies depending on the application. Two basic desiderata are regulation and command tracking these refers to how well the controlled variable tracks the desired value. Specific criteria for command tracking include rise time and settling time. Some processes must not allow an overshoot of the process variable beyond the set point if for example this would be unsafe. Other processes must minimize the energy expended in reaching a new set point.

4.6. Tuning methods

There are several methods for tuning a PROPORTIONAL INTEGRAL DERIVATIVE loop. The most effective methods generally involve the development of some form of process model and then choosing P I and D based on the dynamic model parameters. Manual tuning methods can be relatively inefficient particularly if the loops have response times on the order of minutes or longer. The choice of method will depend largely on whether or not the loop can be taken "offline" for tuning and the response time of the system. If the system can be taken offline the best tuning method often involves subjecting the system to a step change in input measuring the output as a function of time and using this response to determine the control parameters.

4.6.1 Manual tuning

If the system must remain online one tuning method is to first set K_i and K_d values to zero. Increase the K_p until the output of the loop oscillates then the K_p should be set to approximately half of that value for a "quarter amplitude decay" type response. Then increase K_i until any offset is correct in sufficient time for the process too much K_i will cause instability. Finally increase K_d if required until the loop is acceptably quick to reach its reference after a load disturbance. But too much K_d will cause excessive response and overshoot. A fast proportional integral derivative loop tuning usually overshoots slightly to reach the set point more quickly. Some systems cannot accept overshoot in which case an over-damped closed-loop system is required which will require a K_p setting significantly less than half that of the K_p setting causing oscillation.

Table 4.1: Effects of increasing a parameter independently

Parameters	Rise time	Overshoot	Setting time	Steady state error	Stability
K_i	Decrease	Increase	Decrease	Decrease	Degrade
K_p	Decrease	Increase	Decrease	Decrease	Degrade
K_d	Minor Decrease	Minor Decrease	Minor Decrease	No effect in theory	Improve if K_d Small

b) Ziegler–Nichols method

Another heuristic tuning method is formally known as the Ziegler–Nichols method introduced by John G. Ziegler and Nathaniel B. Nichols. As in the method above the K_i and K_d gains are first set to zero. The P gain is increased until it reaches the ultimate gain K_u at which the output of the loop starts to oscillate. K_u and the oscillation period P_u are used to set the gains as shown:

Table 4.2: Ziegler–Nichols method

Controller	K_p	K_i	K_d
P	$.50K_u$	-----	-----
PI	$.45K_u$	$1.2K_p/P_u$	-----
proportional integral derivative	$.60K_u$	$2 K_p/P_u$	$K_p/P_u \delta$

The closed – loop Ziegler-Nichols method consist of following steps.

1. With P-only closed loop control increase the magnitude of the proportional gain until the closed loop is in a continuous oscillation. For slightly larger values of controller gain the closed loop system is unstable while the slightly lower values the system is stable.
2. The value of controller proportional gain that causes the continuous oscillation is called the critical gain K_u . The peak- to - peak period is called critical period P_u .
3. Depending upon controller chosen P PI or PROPORTIONAL INTEGRAL DERIVATIVE use the value in table 3.2 fortuning parameters based on the critical gain and period.

4.7 PROPORTIONAL INTEGRAL DERIVATIVE in proposed model

The characteristic equation $(1+G(s)H(s) = 0)$ in this case is obtained as below:

$$10s^3 + 5.01s^2 + .401s + .00315k = 0$$

Now in this a Routh Hurwitz criterion is applied to determine that value of K (Gain) for which the system shows sustained oscillation or marginal stability. Now by applying this criterion the value of the gain obtained is

$$K = 63.7781 \tag{25}$$

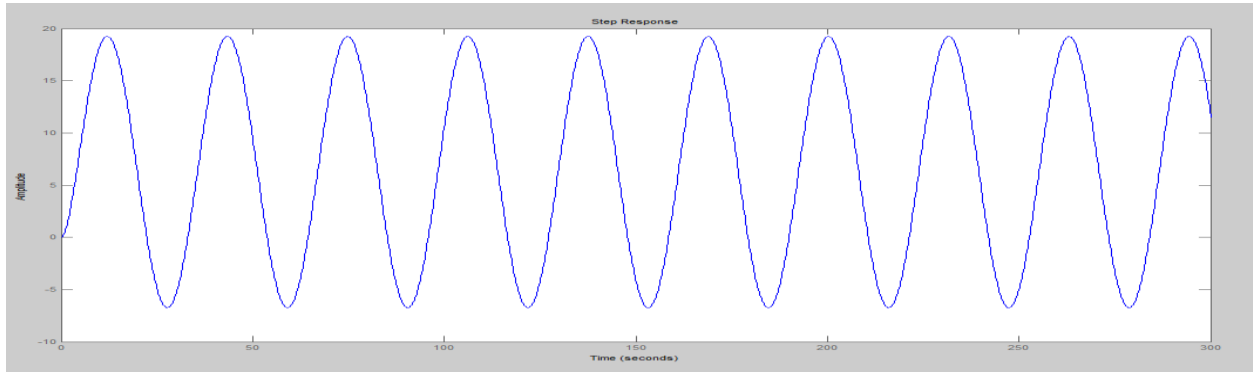


Fig4.3 the step response of the process at the value of gain (k) = 63.7781

A simulation with loop gain $k=63.7781$ shows the process is marginally stable this is the reason

The system shows the sustained oscillations which determine the marginal stability at the particular value of gain.

$$\text{Auxiliary equation } 5.01s^2 + .00315K_C = 0 \quad (26)$$

By putting $s=j\omega$ and the value of gain $K_C = 63.7781$ in equation 28 we get

$$T = 31.389 \text{ and } \omega = .20 \quad (27)$$

The obtained value from the auxiliary equation will help in determining the tuning parameters of Ziegler Nichols method.

Table 4.3 Z-N tuning parameters for Proportional integral derivative

Tuning method	k_c	T_i	T_d
Ziegler-Nichols method	$.6K_C$	$.5T$	$.125T$

For the Proportional integral derivative controller the values of parameters ($K_c \tau_i \tau_d$) obtained using closed loop Oscillation based tuning methods like Zeigler-Nichols method.

TUNING METHOD	K_c	T_i	T_d
Ziegler-Nichols method	38.26	15.69	7.97

In this case study we have taken the parameters tuned using Zeigler-Nichols method. Usually initial design values of proportional integral derivative controller obtained by all means needs to be adjusted repeatedly through computer simulations until the closed loop system performs desired. Figure 4.3 shows the Simulink model of feedback control of solar tracking system. The feedback control is achieved using proportional integral derivative controller.

In this proposed system the disturbance due to wind cloud and rain is considered which is of first order second order and third order respectively. Each model along with disturbances is implemented in Simulink.

4.8 Simulation of feedback controller with different kind of disturbances

4.8.1 Proportional integral derivative controller with first order disturbance

In this the feedback controller is implemented along with the first order disturbance and its effect on the stability is shown by applying unit step and then unit step response is analyzed. The feedback controller model is implemented in simulink and is shown in fig 4.3.

The transfer function of the disturbance due to wind is given as

$$G_{\text{dwind}} = \frac{1}{2s+1} \quad (28)$$

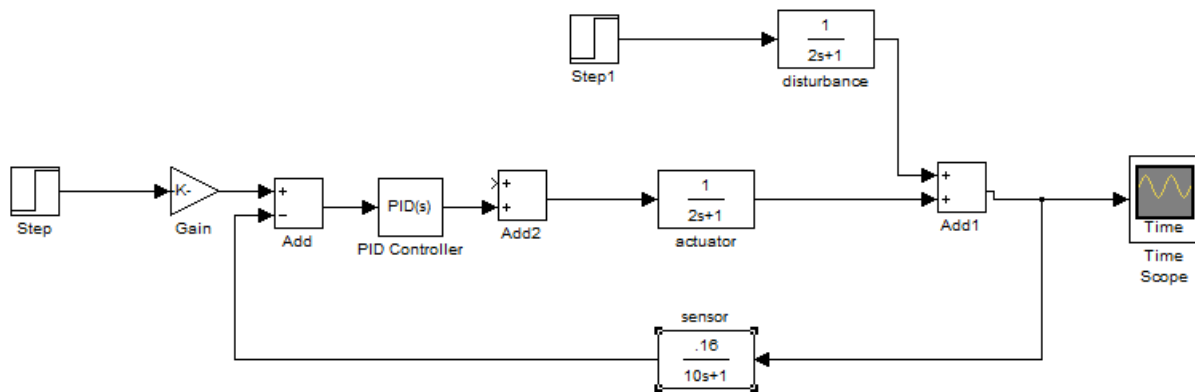


Fig4.3 simulink model with Proportional integral derivative controller with first order disturbance

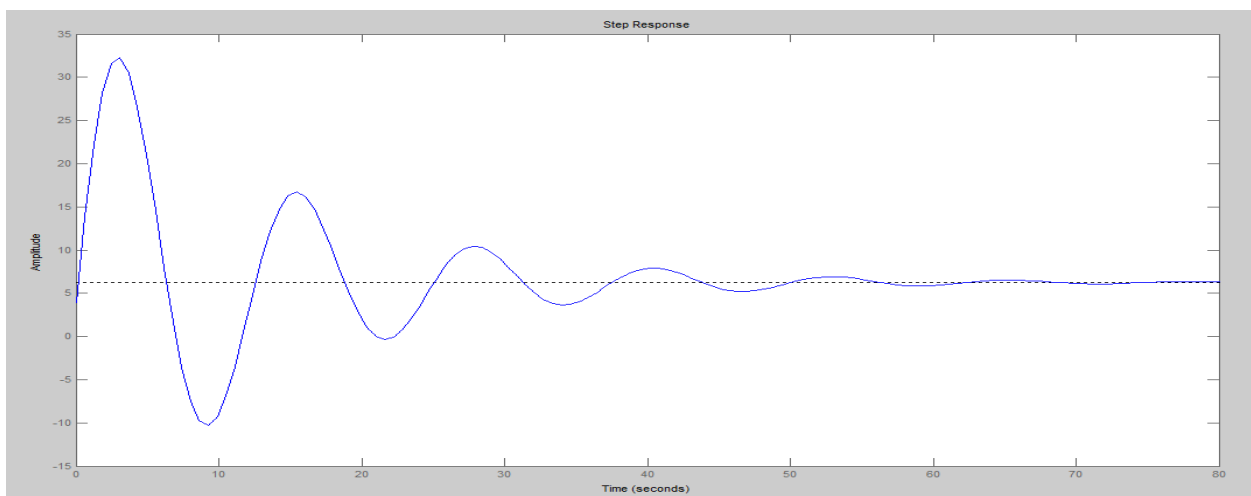


Fig 4.4 Unit step response of the simulation

Rise time = 6.1sec

Settling time = 67.4 sec

4.8.2 Proportional integral derivativewith second order disturbance

In this the feedback controller is implemented along with the second order disturbance and its effect on the stability is shown by applying unit step and then unit step response is analyzed. The feed back controller model is implemented in simulink and is shown in fig 4.5.

$$G_{dcloud} = -.746/s(s+.401) \quad (29)$$

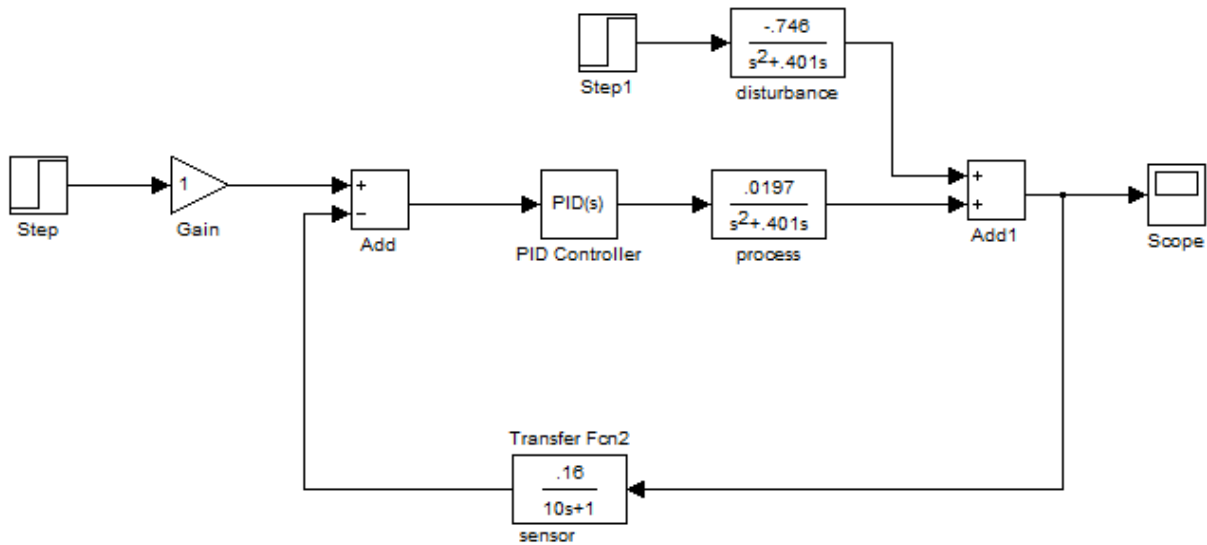


Fig 4.5 Simulink model of Proportional integral derivativewith third order disturbance

4.8.3 Proportional integral derivativewith third order disturbance

In this the feedback controller is implemented along with the third order disturbance and its effect on the stability is shown by applying unit step and then unit step response is analyzed. The feed back controller model is implemented in simulink and is shown in fig 4.5.

$$G_{drain} = -.0197/s(s^2+.401)$$

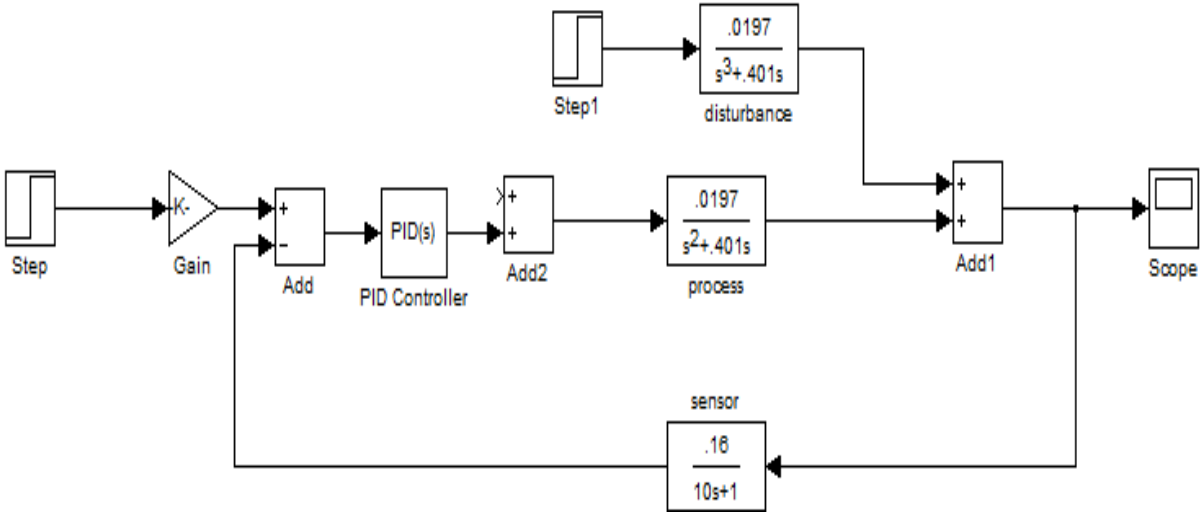
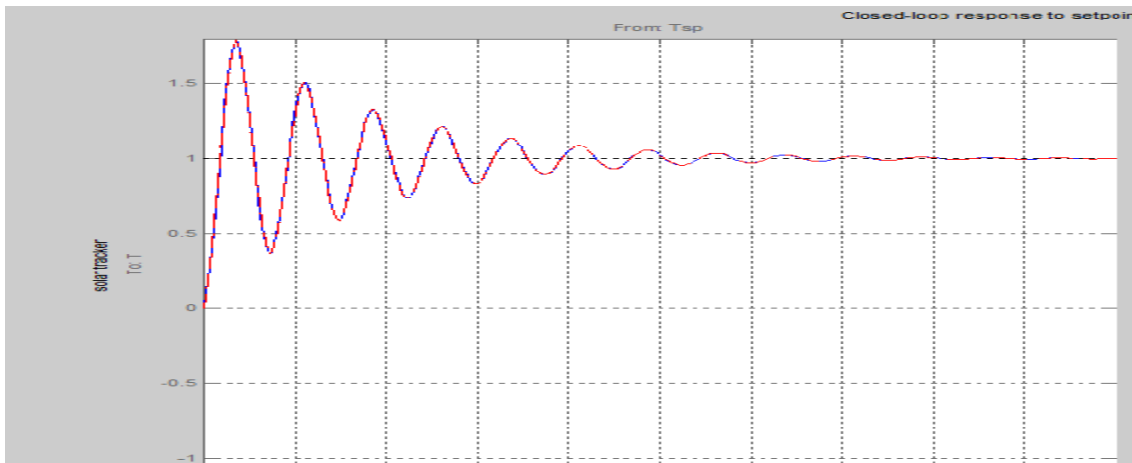


Fig4.6 proportional integral derivativewith third order disturbance

Figure 4.7 shows the unit step response of feedback control of solar tracking system.



Rise time = 3.63 sec

Settling time = 87 sec

Figure 4.7 Simulink model of Proportional integral derivativecontroller with third order disturbance

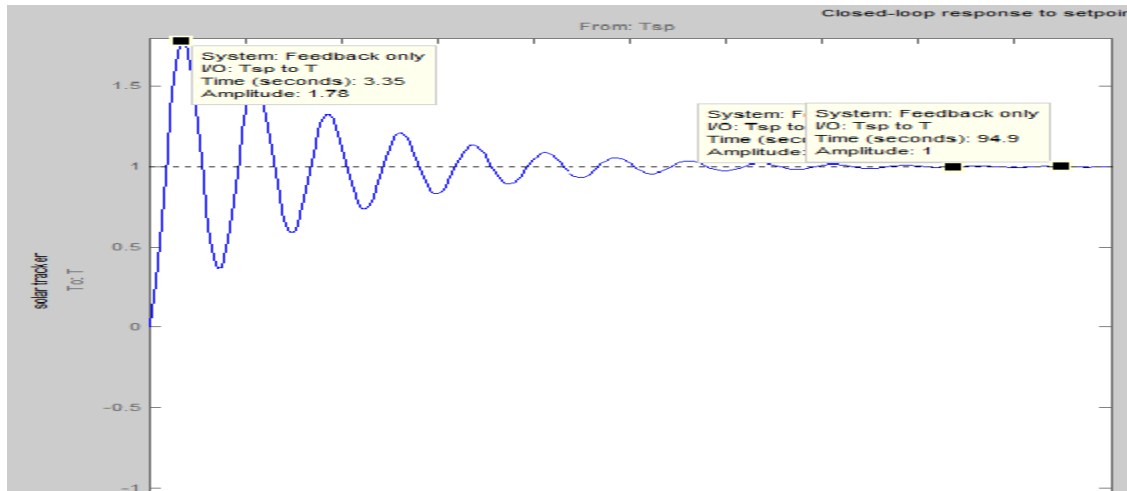


Fig 4.8 unit step response of Simulink model 4.6

Rise time = 3.35 sec

Settling time = 94.2 sec

As the order of the disturbances increases the rise time decreases but the settling time and oscillations increase, which shows the poor performance of the system, which is unacceptable for system performance. To avoid this, a feed forward plus feedback controller is implemented in the next section.

4.9 Feed forward Controller Plus feedback controller

In this section, the feed forward and feedback controller is designed. Because of high overshoot and high settling time, the system performance is considered poor. In order to avoid poor performance, the feed forward controller is added to the system. The feed forward controller is added to the proposed model to reject the effect of disturbances in an acceptable manner. The control action of feedback and feed forward controller is summed up to give a combined control signal. The combined control signal improves the controller performance. In this control scheme, the effect of disturbance is measured and controlled through the feed forward controller. In a feedback control scheme, the sensor is used to detect the process output and gives the error to the controller, which in turn takes appropriate controlling action. But till the controlling action reaches the process, the output has been changed. A feed forward control estimates the error and changes the manipulating variable before the disturbance can affect the output.

The transfer function of the feed-forward controller is $= -G_d f / G_p s$

4.9.1 Feed forward plus feedback system for first order disturbance

In this the feedback controller plus feedforward controller is implemented along with the first order disturbance and its effect on the stability is shown by applying unit step and then unit step response is analyzed. The feed back plus feedforward controller model is implemented in simulink and is shown in fig 4.8.

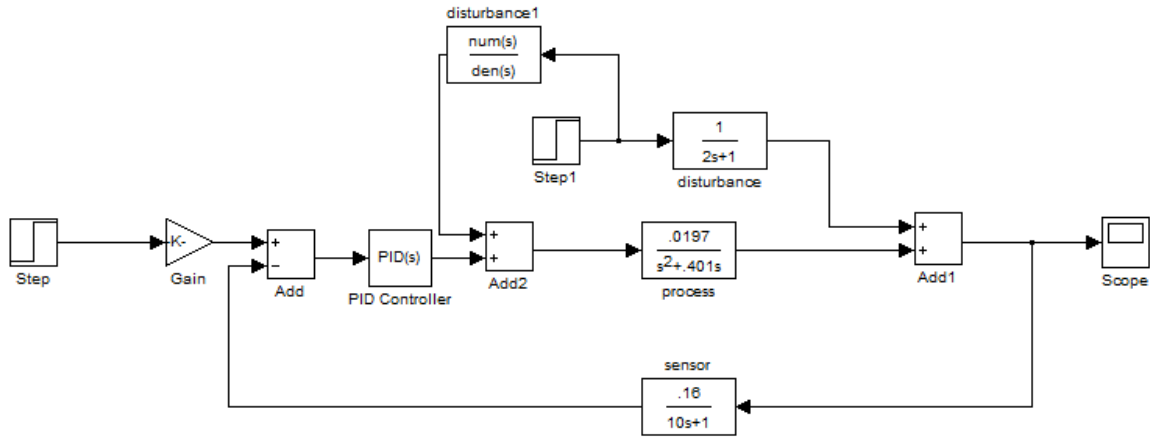


Fig 4.9 feed forward controller for first order disturbance

the feedforward controller cannot be implemented for the first order disturbance because the order of denominator must be greater than the order of numerator.

4.9.2 Feed forward controller for second order disturbance

In this the feedback controller plus feedforward controller is implemented along with the second order disturbance and its effect on the stability is shown by applying unit step and then unit step response is analyzed. The feed back controller model is implemented in simulink and is shown in fig 4.10

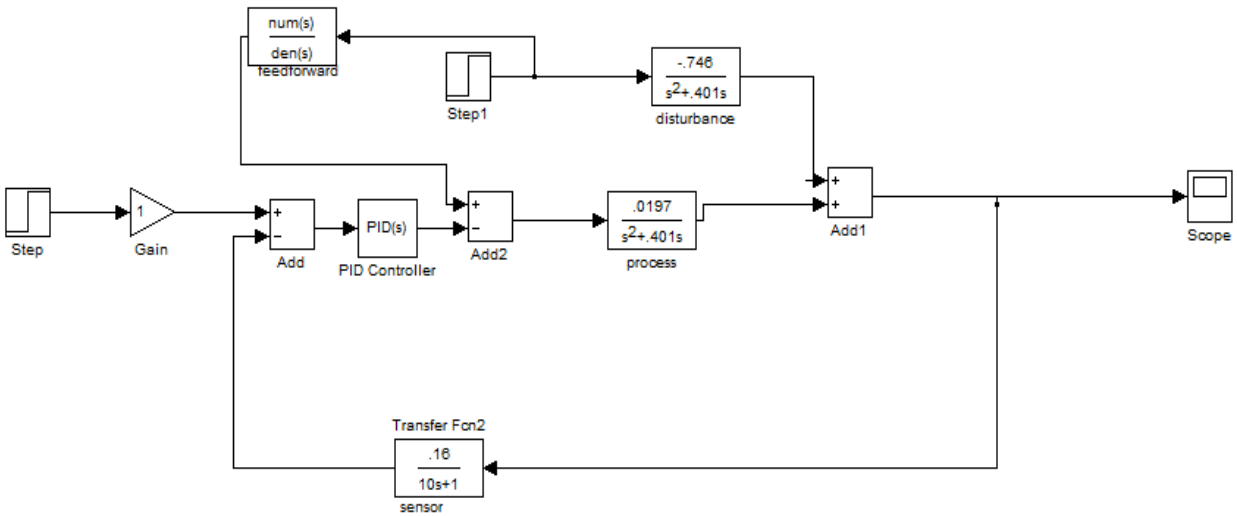


Fig4.10 Simulink model of feedback plus feed forward controller

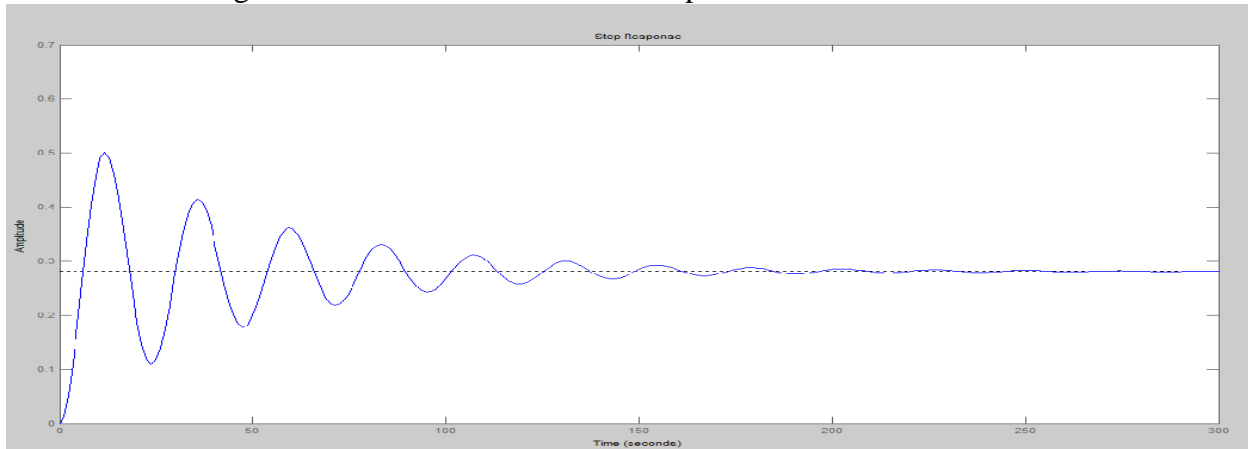


Figure 4.11 shows the unit step response of feedback plus feed forward controller.

Rise time = 3.1 sec

Settling time = 71.4 sec

By applying the feedforward controller the rise time and settling time and the amplitude of system response decreases hence shows the improved system stability

4.9.3 Feed forward controller for third order disturbance

In this the feedback controller is implemented along with the third order disturbance and its effect on the stability is shown by applying unit step and then unit step response is analyzed. The

feed back controller model is implemented in simulink and is shown in fig 4.11

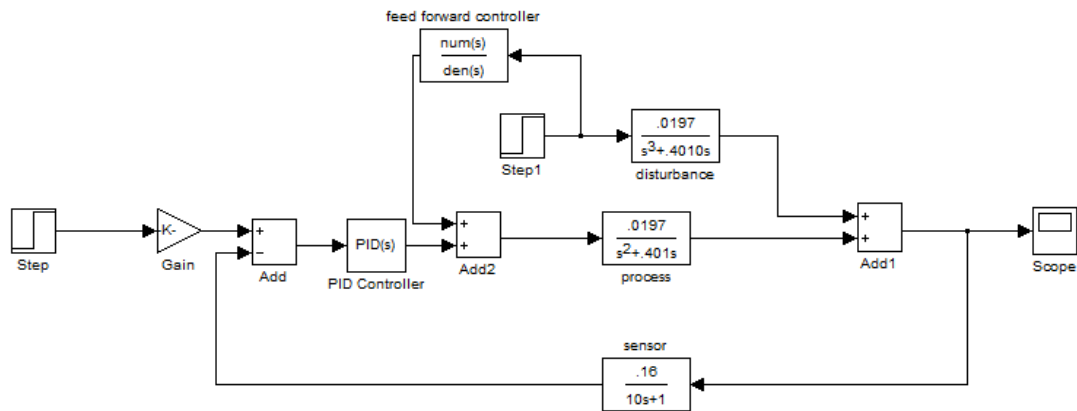


Fig 4.11 simulink model of feed forward controller with third order disturbance

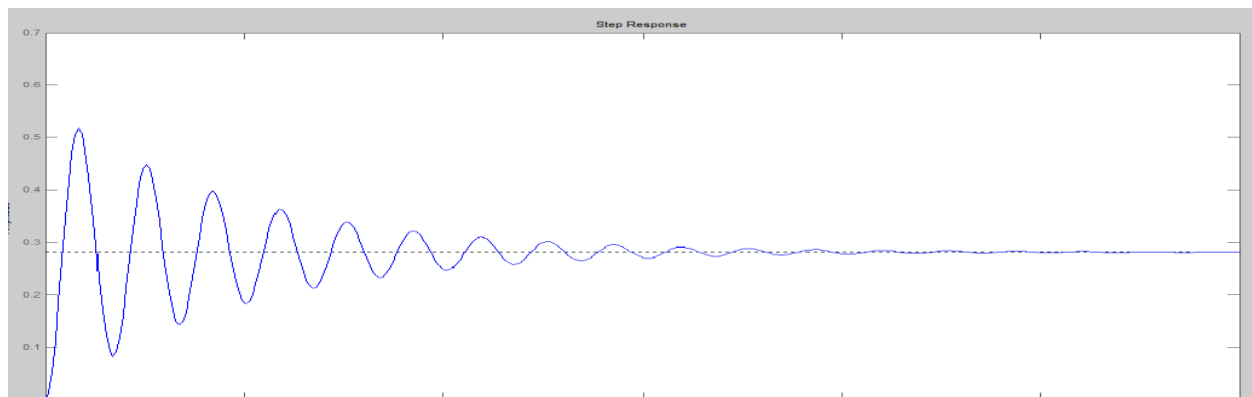


Figure 4.13 the step response of feedback plus feed forward controller with a third order system

Rise time = 3.4 sec

Settling time = 70 .1 sec

The designed feedback plus feed forward controller also shows less overshoot which is an improvement from the feedback controller in all the three cases of disturbances. The feedback controller showed unacceptable overshoot and the feedback plus feed forward controller reduced

the overshoot to appropriate level. Still there is overshoot which can be reduced to a desired level by the use of Internal Modal Controller which is described in next chapter.

IMC AND ITS IMPLEMENTATION FOR PROPOSED SYSTEM

INTRODUCTION

The Internal Model Control (IMC) philosophy relies on the Internal Model Principle which states that control can be achieved only if the control system encapsulates either implicitly or explicitly some representation of the process to be controlled. In particular if the control scheme has been developed based on an exact model of the process then perfect control is theoretically possible. Consider for example the system shown in the diagram below

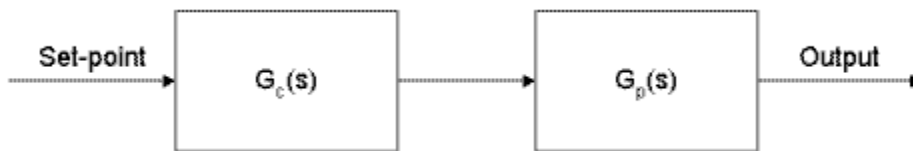


Fig 5.1 Open loop control strategy

A controller $G_c(s)$ is used to control the process $G_p(s)$. Suppose $\bar{G}_p(s)$ is a model of $G_p(s)$. By setting $G_c(s)$ to be the inverse of the model of the process

$$G_c(s) = \bar{G}_p(s)^{-1} \tag{31}$$

And if $G_c(s) = \bar{G}_p(s)$ the model is considered an exact representation of the process

Then it is clear that the output will always be equal to the set point. This ideal control performance is achieved without feedback. This also described that if there is complete knowledge about the process being controlled perfect control can be easily achieved. It also described that feedback control is necessary only when knowledge about the process is inaccurate or incomplete.

5.2 The IMC Strategy

Practically process-model mismatch is common; the process model may not be invertible and the system is often affected by unknown disturbances. Thus the above open loop control arrangement will not be able to maintain output at set point. Nevertheless it forms the basis for the development of a control strategy that has the potential to achieve perfect control. This strategy known as Internal Model Control (IMC) has the general structure depicted in Fig. 5.2

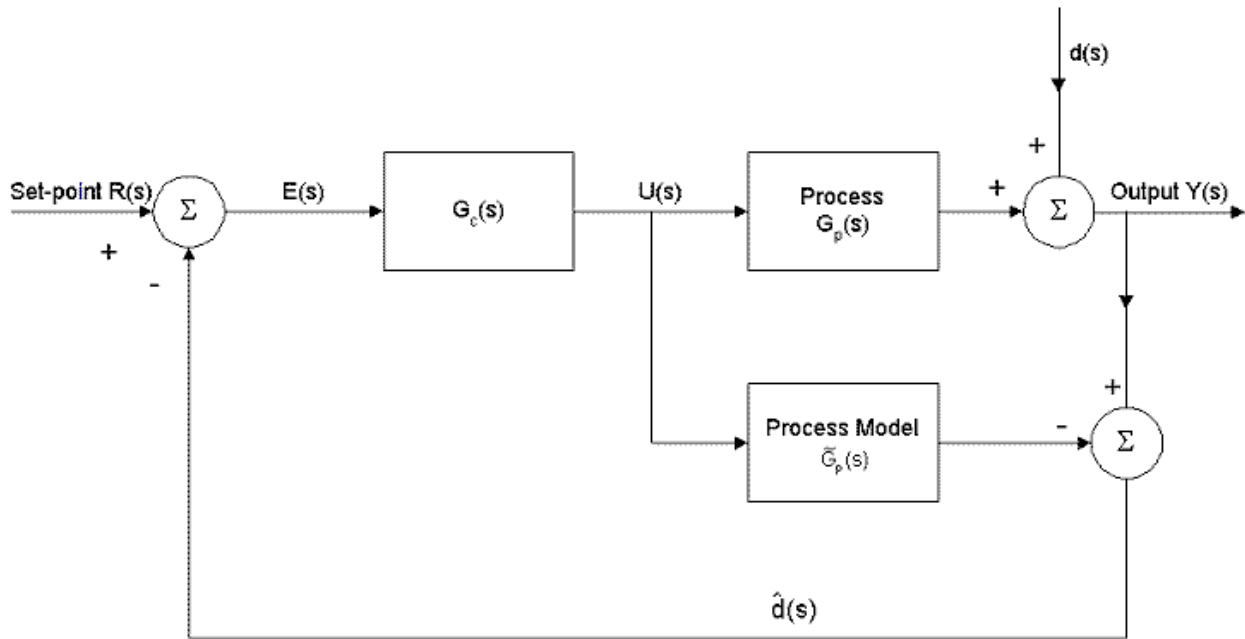


Fig 5.2 Schematic of the IMC scheme

In the diagram $d(s)$ is an unknown disturbance affecting the system. The manipulated input $U(s)$ is introduced to both the process and its model. The process output $Y(s)$ is compared with the output of the model resulting in a signal $\hat{d}(s)$. That is

$$\hat{d}(s) = [G_p(s) - \bar{G}_p(s)^{-1}]U(s) + d(s) \quad (32)$$

If $d(s)$ is zero for example then $\hat{d}(s)$ is a measure of the difference in behavior between the process and its model. If $G_p(s) = \bar{G}_p(s)$ then $\hat{d}(s)$ is equal to the unknown disturbance. Thus $\hat{d}(s)$ may be regarded as the information that is missing in the model and can therefore be used

to improve control. This is done by subtracting $d^{\wedge}(s)$ from the set point $R(s)$ which is very similar to affecting a set point trim. The resulting control signal is given by

$$U(s) = [R(s) - d^{\wedge}(s)] G_c(s) = \{R(s) - [G_p(s) - \bar{G}_p(s)] U(s) - d^{\wedge}(s)\} G_c(s) \quad (33)$$

$$\text{Then } U(s) = \frac{[R(s) - d(s)] G_c(s)}{[1 + G_p(s) - \bar{G}_p(s)] G_c(s)} \quad (34)$$

$$Y(s) = G_p(s) U(s) + d_p(s) \quad (35)$$

The closed loop transfer function for the IMC scheme is therefore

$$= \frac{[R(s) - d(s)] G_c(s) G_p(s) + d(s)}{[1 + G_p(s) - \bar{G}_p(s)] G_c(s)} \quad (36)$$

From this closed loop expression if $G_p(s) = \bar{G}_p(s)$ and $G_c(s) = \bar{G}_p(s)^{-1}$ then perfect set point tracking and disturbance rejection is achieved.

If $G_p(s) \neq \bar{G}_p(s)$ perfect disturbance rejection can still be realized provided $G_c(s) = \bar{G}_p(s)^{-1}$.

Additionally to improve robustness the effects of process model mismatch should be minimized. Since discrepancies between process and model behavior usually occur at the high frequency end of the system's frequency response a low-pass filter $G_f(s)$ is usually added to attenuate the effects of process-model mismatch. Thus the internal model controller is usually designed as the inverse of the process model in series with a low-pass filter i.e.

$G_{imc}(s) = G_c(s) G_f(s)$. The order of the filter is usually chosen such that $G_c(s) G_f(s)$ is proper to prevent excessive differential control action. The resulting closed loop then becomes

$$Y(s) = \frac{G_{imc}(s) G_p(s) R(s) + [1 - G_{imc}(s) \bar{G}_p(s)] d(s)}{1 + [G_p(s) - \bar{G}_p(s)] G_{imc}(s)} \quad (37)$$

5.3 PRACTICAL DESIGN OF IMC

Designing an internal model controller is relatively easy. Given a model of the process $\bar{G}_P(s)$ first factor $\bar{G}_P(s)$ into "invertible" and "non-invertible" components.

$$\bar{G}_P(s) = \bar{G}_P(s)^- \bar{G}_P(s)^+ \quad (38)$$

The non-invertible component $\bar{G}_P(s)^-$ contains terms which if inverted will lead to instability and realisability problems e.g. terms containing positive zeros and time-delays. Next set $G_c(s) = \bar{G}_P(s)^+{}^{-1}$ and then $G_{imc}(s) = G_c(s)G_f(s)$ where $G_f(s)$ is a low-pass function of appropriate order.

Thus the IMC scheme has the following properties :

- it provides time-delay compensation
- the filter can be used to shape both the set point tracking and disturbance rejection responses
- at the steady-state the controller will give offset free responses

5.4 Implementing the imc within a conventional proportional integral derivative framework

The IMC philosophy can also be used to generate settings for conventional PI or Proportional integral derivative controllers. The IMC block diagram in Fig5.2 can be reduced to a conventional closed loop structure by first re-arranging to the following form

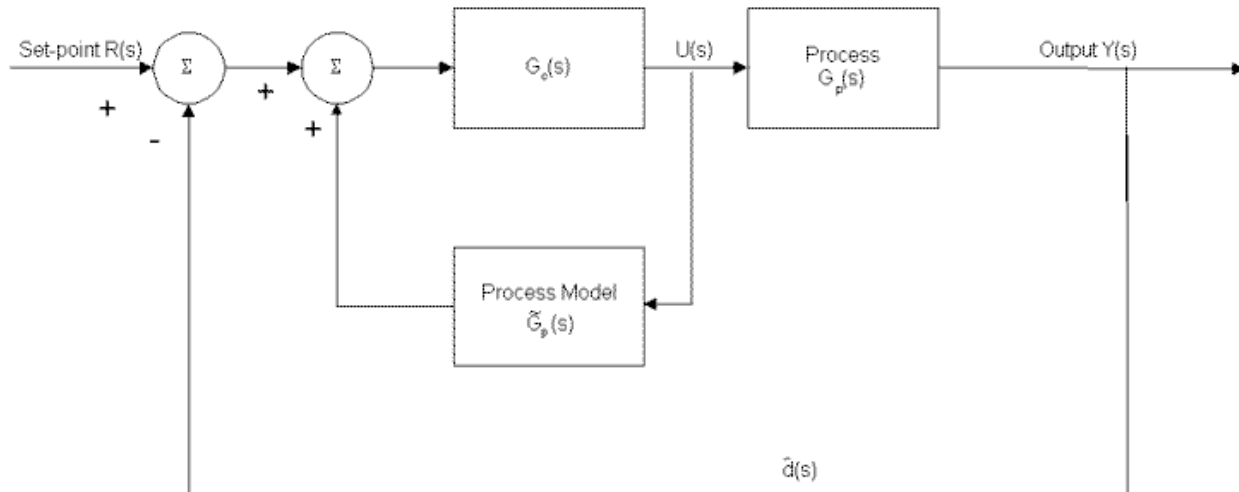


Fig 5.3 shows the rearrangement of imc block diagram

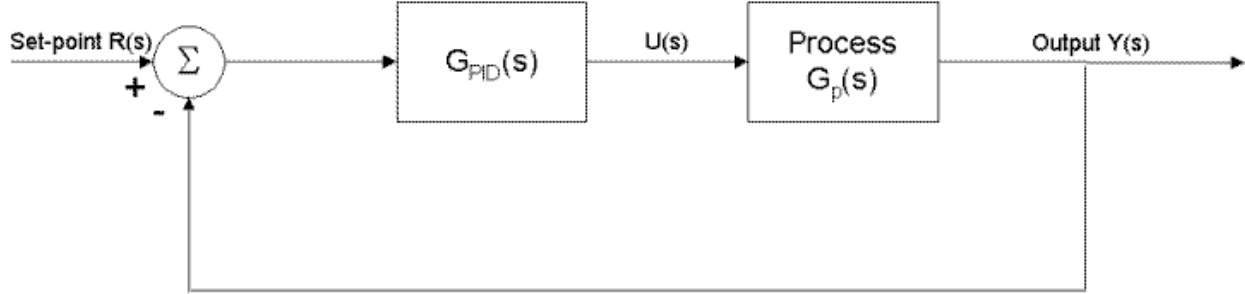


Fig 5.4 IMC reduced to conventional block diagram

$$\text{Thus } G_{\text{PROPORTIONAL INTEGRAL DERIVATIVE}}(s) = \frac{G_{\text{imc}}(s)}{1 - G_{\text{imc}}(s) \bar{G}_p(s)} \quad (39)$$

5.5 IMPLEMENTING IMC FOR THE PROPOSED MODEL

5.5.1 Transfer function of IMC

transfer function of the process is shown in equation (39) .

$$G_p(s) = \frac{.0197}{s(s + .401)} \quad (40)$$

$$f(s) = 1 / (\lambda s + 1) \quad (41)$$

$$G_{\text{imc}}(s) = G_p(s)^{-1} f(s) \quad (42)$$

Take the value of λ as 0.5 which is practically one third of one fifth of time constant and put it in equation (41) to get the value of ideal internal model control controller $Q(s)$. The equation becomes

$$G_{\text{imc}}(s) = \frac{.0197}{s(s+.401)(.5s+1)} \quad (43)$$

now the above calculate transfer function model is implemented in Matlab/Simulink model to know the stability of the proposed model .The Simulink model is implemented as per the schematic architecture of imc.

5.5.2 IMC in proposed process without disturbance

In this the imc is implemented to the proposed system without disturbance and its unit step response is analyzed

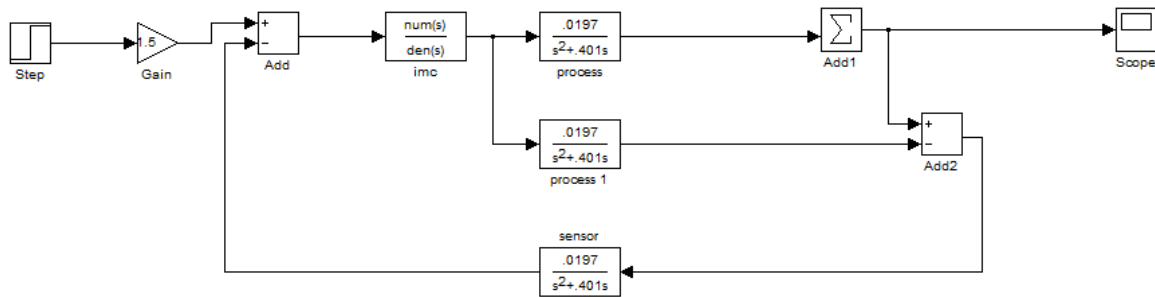


Fig 5.5 imc controller

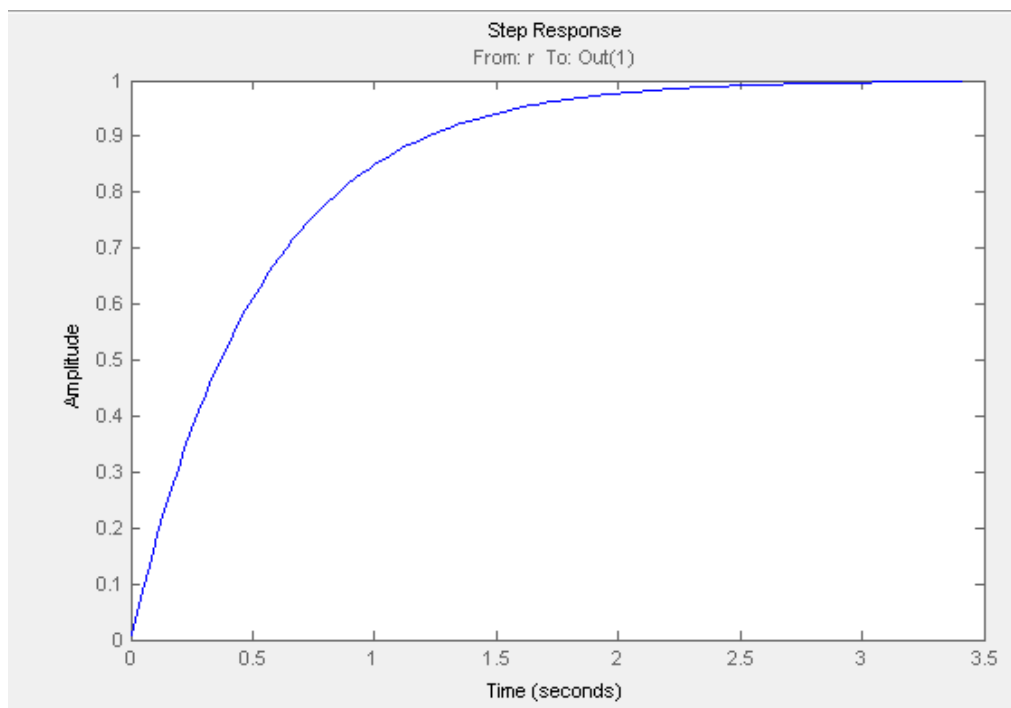


Fig 5.6 unit step response for the ideal imc based system

Unit step response of internal model control based proportional integral derivative controller for the second order system with third order disturbance

5.5.3 IMC controller for the process with first order disturbance

In this the imc is implemented to the proposed system with first order disturbance and its unit step response is analyzed

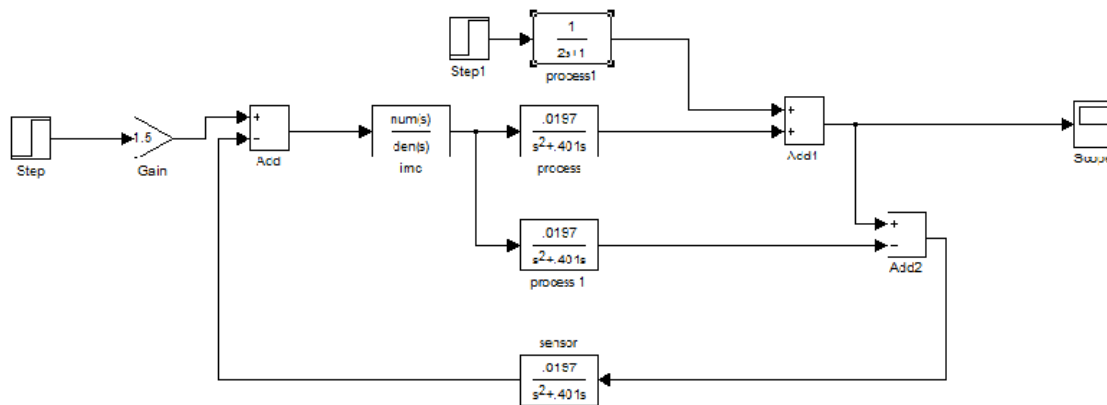


Fig5.7 imc with first order disturbance

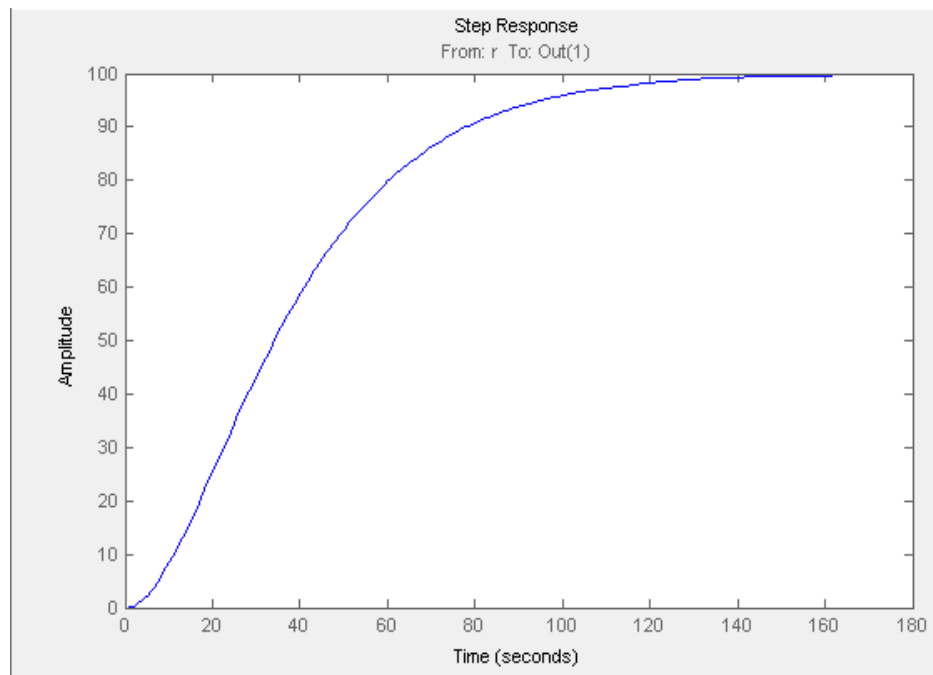


Fig 5.8 unit step response of fig 5.7

5.5.4 IMC for process system with second order disturbance

In this the imc is implemented to the proposed system with second order disturbance and its unit step response is analyzed

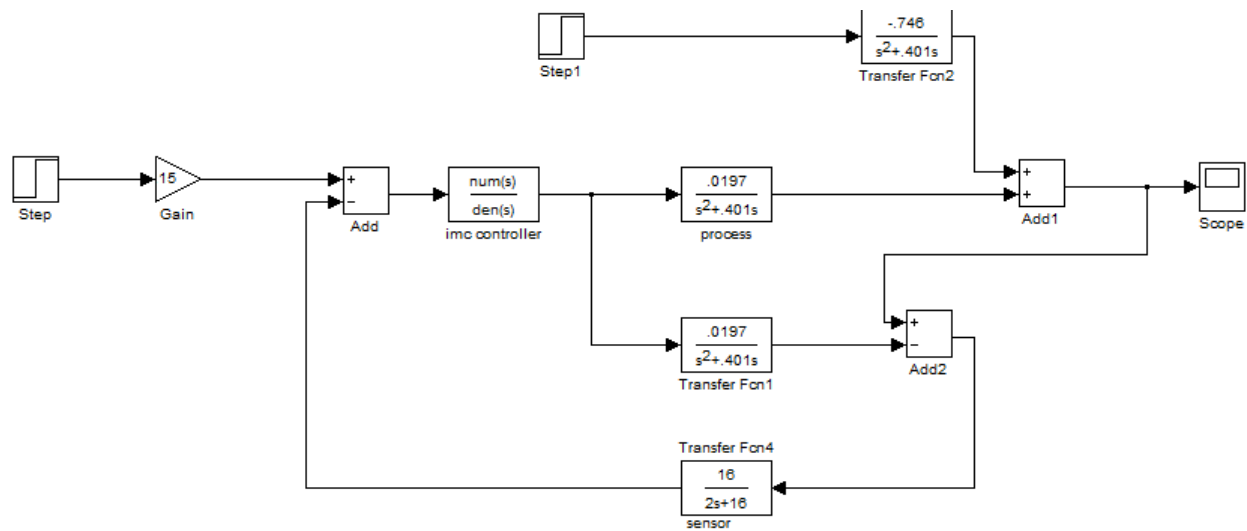


Fig 5.5 Simulink model of IMC for second order disturbance

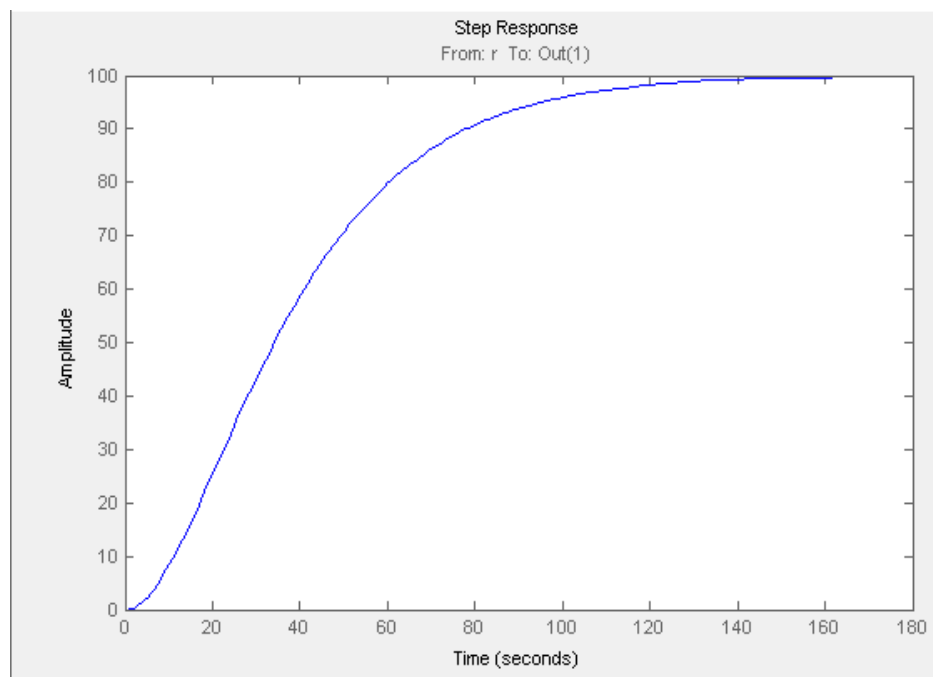


Fig 5.6 unit step response with IMC controller with second order disturbance

Rise time = 4.8 sec settling time = 67.2sec overshoot=0

5.5.5 IMC for the process control for third order disturbance

In this the imc is implemented to the proposed system with third order disturbance and its unit step response is analyzed.

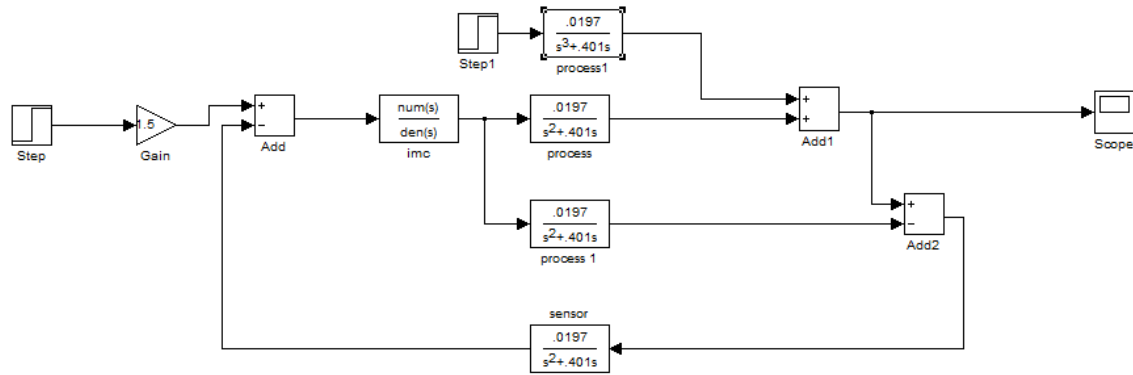


Fig 5.6 IMC controller with third order disturbance

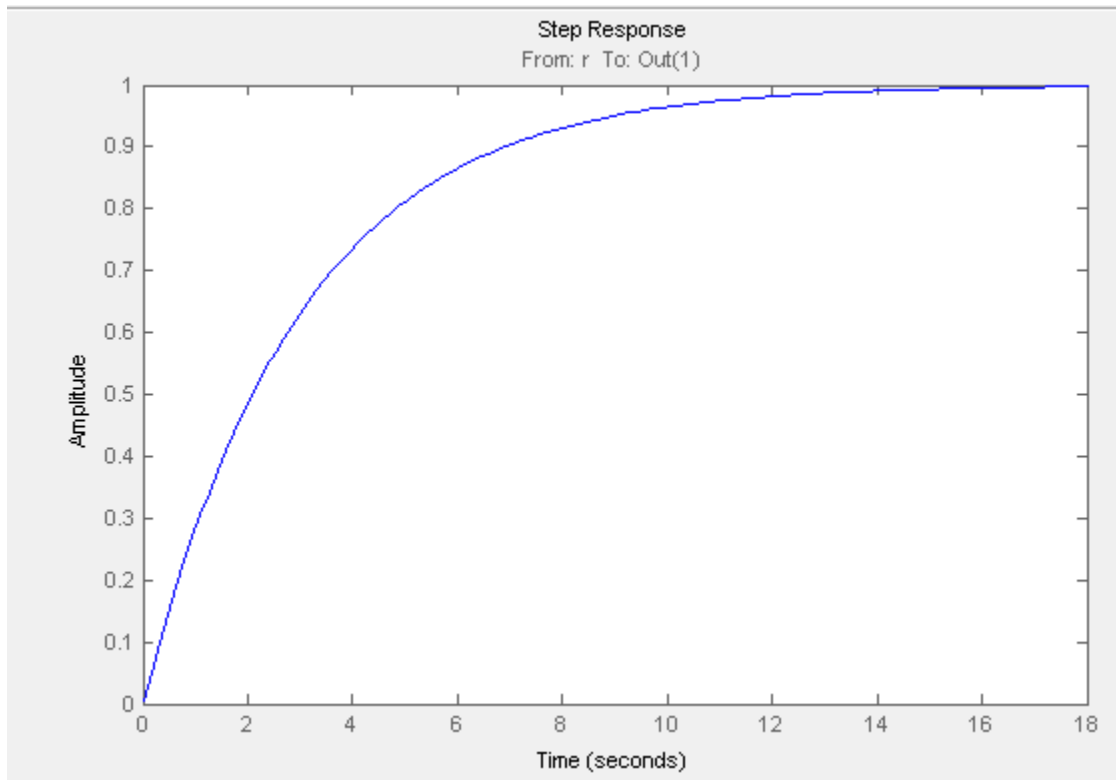


Fig shows the unit step response for the third order disturbance

In this it is shown the unit step response of internal model based controller in solar tracking system with value of filter parameter along with first order, second order and third order disturbance . As the graph shows the maximum overshoot is nearly less than 1% .The designed internal model controller is very much effective because it shows very low overshoot and has only one tuning parameter which is the filter parameter.

RESULTS AND CONCLUSION

In this thesis different conventional controllers are implemented for the stability analysis of solar tracking system with the different orders of disturbances introduced .firstly the proportional integral derivative controller is implemented which shows unacceptable overshoot after that the feed forward controller is implemented which shows the reduced overshoot but still effects the performance of proposed system.

The proportional integral derivative controller shows a peak overshoot of 35- 40% for the first order ,second order and third order disturbances after applying the feed forward plus feedback controller the peak overshoot reduces to 30- 33% for first order, second order and third order disturbances. But it is the model based controller that significantly reduces the peak overshoot and the peak overshoot of IMC is nearly 1% for all the disturbances. It is clear from the step response analysis that the model based controllers give a better control than the conventional feedback and feed forward controllers.

The proportional integral derivative controller gives high peak overshoot and unacceptable settling time. The peak overshoot and oscillations is in a higher side. To compensate the high peak overshoot feed forward controller was designed. The feed forward controller along with feedback controller estimates the error due to disturbances and tries to ease the performance of the designed process system after that the internal model controller reduces the peak overshoot to nearly 1% and reduces the settling time to and rise time.

It is clear that the IMC based controller gives a better control results as compared to feedback and feed forward controller when a unit step input is applied.

CHAPTER 6

CONCLUSION AND FUTURE SCOPE

In this thesis a stability analysis of solar tracking system is performed with the help of different conventional controllers so that it can track maximum solar energy in the shortest possible time and minimum or no overshoot. After time response and frequency response based analysis carried out on different controllers it is observed that IMC controller provides a satisfactory performance in both steady state and transient state and overcomes the drawbacks of conventional proportional integral derivative controller feedback plus feed-forward controller. This demonstrated approximately 100% improvement in the overshoot and better improvement in settling time as compared to the conventional proportional integral derivative controller.

In future scope of the thesis the hybrid fuzzy controller technique can be used to identify and estimate the better performance of the proposed system and fuzzy controller with filters can be used to obtain the membership functions and optimize the existing one.

REFERENCES

- [1] Benjamin C.K. 2010. "Automatic Control System" John Wiley & Sons. Inc.
- [2] Craft A. and R. Davison 1999. "Mathematics for Engineering" Adison Wesley Limited.
- [3] Dune E.R. 1998. "Wind Load Definition for Line- Focus Concentrating Solar Collectors" Sandia National Laboratories Albuquerque NM 8725.
- [4] Fu K.S. R. Gonzalez and C. Lee 1987. "Robotics: Control Sensing Vision and Intelligence." McGraw-Hill Inc.
- [5] Kalogirou S. 1996. "Parabolic trough Collector System for Low Temperature Steam Generation: Design and Performance Characteristics" Applied Energy 55(1): 1-19.
- [6] Knudsen M. and J. Grue 1995. "Estimation of Nonlinear dc Motor Models Using a Sensitivity Approach" Thaird European Control Conference ECC'95 Rome.
- [7] Mohamed A.Z. M.N. Eskander and F.A. Ghali 2001. "Fuzzy Logic Control Based Maximum Power Tracking of Wind Energy System" Renewable Energy 23: 235-245.
- [8] Richard M.C. 1995. "Electric Drives and their Controls" Oxford University Press Inc. New York.
- [9] Saxena A.K. and V. Dutta 1990. "A Versatile Microprocessor Based Controller for Solar Tracking" Conference Record of the Twenty First IEEE Photovoltaic Specialists Conference.
- [10] Simiu E. and R.H. Scanlan 1996. "Wind effects on structures: Fundamental and Applications to design" John Willy & Sons Inc. pp: 135-194.
- [11] Thomas A. 1996. "Solar Steam Generating System Using parabolic trough Concentrators" Energy Conversion and Management 37(2): 215-245.
- [12] William C.D. and N.C. Paul 1980. "Solar Energy Technology Handbook" Marcel Dekker Inc. USA New York.
- [13] Vyacheslav Khavrus and Ihor Shelevytsky Introduction to solar motion geometry on the basis of a simple model Phys. Educ. 45 641-665 2010.
- [14]. Gustavo Ozuna Carlos Anaya. Diana Figueroa. Nun Pitalua Solar Tracker of Two Degrees of Freedom for Photovoltaic Solar Cell Using Fuzzy Logic Proceedings of the World Congress on Engineering London U.K 2011.

- [15]. Ahamed M. Hamed El-Shafei B. Zeidan Ali S. Alosaimy and Talal K. Kassem Application of solar energy for regeneration of liquid desiccant using rotating tilted wick International Journal of Mechanical & Mechatronics Engineering IJMME-IJENS Vol:12 No:05 2012.
- [16]. Wai Phyo Aung Analysis on Modeling and Simulink of DC Motor and its Driving System Used for Wheeled Mobile Robot World Academy of Science Engineering and Technology 32 2007.
- [17]. Richard C. Dorf and Robert H. Bishop. Modern Control Systems. Ninth Edition Prentice-Hall Inc. New Jersey 2001.
- [18] Nobuhiro Yokoyama ,Yoshimasa Ochi, "PID Controller Design for MIMO Systems by Applying Balanced Truncation to Integral-Type Optimal Servomechanism", IFAC Conference on Advances in PID Control PID'12 Brescia (Italy), March 28-30, 2012

